

2012

Evaporative losses from a common reed- dominated peachleaf willow and cottonwood riparian plant community

Isa Kabenge

Makerere University

Suat Irmak

University of Nebraska-Lincoln, suat.irmak@unl.edu

Follow this and additional works at: <http://digitalcommons.unl.edu/biosysengfacpub>



Part of the [Bioresource and Agricultural Engineering Commons](#), [Environmental Engineering Commons](#), and the [Other Civil and Environmental Engineering Commons](#)

Kabenge, Isa and Irmak, Suat, "Evaporative losses from a common reed-dominated peachleaf willow and cottonwood riparian plant community" (2012). *Biological Systems Engineering: Papers and Publications*. 478.
<http://digitalcommons.unl.edu/biosysengfacpub/478>

This Article is brought to you for free and open access by the Biological Systems Engineering at DigitalCommons@University of Nebraska - Lincoln. It has been accepted for inclusion in Biological Systems Engineering: Papers and Publications by an authorized administrator of DigitalCommons@University of Nebraska - Lincoln.

Evaporative losses from a common reed-dominated peachleaf willow and cottonwood riparian plant community

Isa Kabenge¹ and Suat Irmak²

Received 22 January 2012; revised 26 June 2012; accepted 11 July 2012; published 11 September 2012.

[1] Our study is one of the first to integrate and apply within-canopy radiation physics parameters and scaling-up leaf-level stomatal resistance (r_L) to canopy resistance (r_c) approach to quantify hourly transpiration (TRP) rates of individual riparian plant species—common reed (*Phragmites australis*), peachleaf willow (*Salix amygdaloides*), and cottonwood (*Populus deltoides*)— in a mixed riparian plant community in the Platte River Basin in central Nebraska. Two experimental years (2009 and 2010) were contrasted by warmer air temperature and presence of flood water in 2010. The seasonal average r_c values for common reed, peachleaf willow, and cottonwood in 2009 were 76, 70, and 107 s m⁻¹, respectively. The corresponding r_c values in the flood year (2010) were 70, 66, and 105 s m⁻¹ for the same species, respectively. In 2009, the seasonal total TRP for common reed, peachleaf willow, and cottonwood were 483, 522, and 431 mm, respectively. Corresponding TRP values in 2010 were greater as 550, 655, and 496 mm, respectively. In 2009, TRP accounted for 64% of ET_a during June–September, and the proportion varied between 41% and 69% for most of the season. In 2010, TRP accounted for 61% of ET_a during June–September, and the proportion varied between 41% and 65% for most of the season. The average surface evaporation rate of the riparian zone was 0.81 mm d⁻¹ in 2009 and 1.70 mm d⁻¹ in 2010. Seasonal evaporation was 160 mm in 2009 and 312 mm in 2010. The study provides a basis for understanding the dynamics of transpiration for riparian vegetation in response to the environmental conditions and provides valuable water use data for more complete water balance analyses by accounting for the water use of riparian vegetation species.

Citation: Kabenge, I., and S. Irmak (2012), Evaporative losses from a common reed-dominated peachleaf willow and cottonwood riparian plant community, *Water Resour. Res.*, 48, W09513, doi:10.1029/2012WR011902.

1. Introduction

[2] Decline in availability of freshwater resources, assessment, allocation, management, and use have become critical issues for agroecological settings and other natural systems in Nebraska, in other Midwestern states, and around the world. Thus, quantification of water use rates for various vegetation surfaces, including riparian systems, is becoming more important for accounting for water use of these systems in the local and regional water balance analyses. Accurate quantification of evaporative fluxes from riparian zones can also aid water resources managers and decision makers developing effective water allocation programs on a catchment or watershed scale. Wetlands and riparian zones are significant water users and cover large areas of the Earth's surface. For a particular region, native and nonnative

riparian species usually coexist in a balanced ecosystem and provide various important functions of the riparian zones, including storage for flood water, habitat for fauna and flora [Blossey *et al.*, 2002; Lafleur, 2008], and various economic and other environmental benefits. Among the many species, cottonwood and peachleaf willow are some of the dominant species in many riparian areas in the United States, and nonnative plant species (i.e., common reed) are known to rapidly invade riparian areas and alter the ecosystem functions [Blossey, 1999; Amsberry *et al.*, 2000; Blossey *et al.*, 2002; Mal and Narine, 2004; Knezevic *et al.*, 2008]. Invasive riparian systems may also alter the rates of ecosystem CO₂ exchange and ecosystem evaporative losses and water use efficiency [Potts *et al.*, 2008]. For example, similar to woody encroachment in some semiarid ecosystems, it was observed that *Cynara* (*Cynara cardunculus*; cardoon or artichoke thistle) invasion increases midday ecosystem CO₂ assimilation and evapotranspiration rates and has the potential to increase C storage in California coastal grasslands [Potts *et al.*, 2008]. The impact of invasive plant infestations, e.g., pepperweed (*Lepidium latifolium* L.) on net CO₂ exchange measured continuously at the ecosystem scale was recently investigated by Sonnentag *et al.* [2011], who analyzed how the pepperweed flowering and control measures such as mowing affect canopy photosynthesis and autotrophic respiration and ecosystem respiration. They found that

¹College of Agricultural and Environmental Sciences, Makerere University, Kampala, Uganda.

²Department of Biological Systems Engineering, University of Nebraska-Lincoln, Lincoln, Nebraska, USA.

Corresponding author: S. Irmak, Department of Biological Systems Engineering, University of Nebraska-Lincoln, 239 L. W. Chase Hall, Lincoln, NE 68583, USA. (sirmak2@unl.edu)

This paper is not subject to U.S. copyright.

Published in 2012 by the American Geophysical Union.

unmoved pepperweed caused the site to be almost CO₂ neutral in 2007 (as $-28 \text{ g C m}^{-2} \text{ period}^{-1}$) or a net source in 2009 (as $129 \text{ g C m}^{-2} \text{ period}^{-1}$), mostly because of reduced maximum photosynthetic capacity. They observed that mowing during early flowering reversed the attenuating effects of pepperweed, causing the site to act as a net CO₂ sink in 2008 (as $-174 \text{ g C m}^{-2} \text{ period}^{-1}$) mainly due to prolonged photosynthetic CO₂ uptake over the plant's early vegetative growth phase.

[3] Wetlands and riparian systems in the Platte River Valley and the mainland United States as a whole have been invaded by nonnative common reed that outcompetes most of the native plants, changes the wetland hydrology, alters wildlife habitat, and increases fire danger [Blossey, 1999; Amsberry et al., 2000; Blossey et al., 2002; Mal and Narine, 2004; Knezevic et al., 2008]. The state of Nebraska designated common reed as a noxious weed, legally defined as "a destructive or harmful pest." Concern about the spreading of common reed, peachleaf willow, and cottonwood along the river banks, wetlands, and other water bodies as well as their impact on water balances in Nebraska requires accurate quantification of water use rates for riparian zones so that the availability and use of freshwater resources by various vegetation types can be determined and accounted for in the planning, managing, and allocating water resources in the region. The state of Nebraska has interest in the hydrological regime and magnitude of water fluxes of the riparian species because their continued increase in water use may lead to insufficient water from the Platte River to meet future water needs, especially for irrigation and other natural habitat functions. In many regions, including Nebraska, there is a lack of information on water use data for native and invasive riparian plant species, including common reed, which is a typical invasive riparian species found in Nebraska. In an effort to address long-term water resources challenges, the Nebraska State legislators passed legislation, which is a new vehicle to reduce water use of invasive species by removal or control via spraying or other methods to reduce or eliminate their water use from the hydrological system. However, while removal of invasive species from the system might contribute to increased water availability to a given riparian ecosystem, the quantity of this contribution is not known. Quantification of water use of individual species before removal will enable decision/policy makers to have information to make better impact assessment of vegetation removal on the water balance in a given watershed. Furthermore, after removal, some other invasive and/or native vegetation can potentially take over the riparian areas. Thus, research projects that run long enough to measure the water use of various species before and after removal in the same area are necessary. This project is designed to run for at least 10 years to quantify and evaluate the aforementioned challenges.

[4] Various methods have been used to quantify riparian vegetation evapotranspiration (ET), including water balance approach and sap flow measurement [Goodrich et al., 2000; Schaeffer et al., 2000; Nagler et al., 2003, 2005, 2007], eddy covariance method [Nagler et al., 2005; Cleverly et al., 2006], and Bowen ratio energy balance system [Drexler et al., 2004; Peacock and Hess, 2004; Nagler et al., 2005; Irmak, 2010]. Most riparian zone studies estimate evaporative fluxes by assuming a uniform vegetative surface instead of considering the complex mosaic nature of the vegetation

species. Thus, in a mixed plant community, most studies provide water use rate data for a mixed riparian vegetation community and rarely report water use rates of specific species. While various methods are currently used to quantify average ET losses from riparian plant communities, these techniques may not be sufficient or practical to use to quantify the evaporative losses of individual species when the riparian system is composed of mixed plant communities. The one-step application of Jarvis-type models [Jarvis, 1976; Jarvis and McNaughton, 1986] coupled with the Penman-Monteith (PM) [Monteith, 1965] type combination-based energy balance approach [Irmak and Mutiibwa, 2010] can provide a robust alternative to quantify ET losses from individual species in the mixed riparian systems. Direct application of this approach relies on measured direct feedback from the individual plant species and measured microclimatic and environmental parameters. This approach involves measurement or modeling of stomatal resistance (r_L) and other primary environmental variables and requires scaling up r_L to canopy resistance (r_c) using microclimatic and plant factors such as leaf area index (LAI) for sunlit and shaded leaves, solar zenith angle, direct and diffuse solar radiation above and within the canopy, and other environmental parameters [Kaufman, 1982; Jarvis and McNaughton, 1986; Rochette et al., 1991; Lhomme et al., 1998; Jones, 1992; Tourula and Heikinheimo, 1998; Furon et al., 2007; Irmak et al., 2008; Irmak and Mutiibwa, 2010; Mutiibwa and Irmak, 2011]. The scaling-up process primarily relies on scaling up r_L to r_c as a function of solar radiation, net radiation, or photosynthetic photon flux density (PPFD). While this approach has been shown to be robust and very accurate in quantifying evaporative losses from croplands, its use in practical application for quantification of evaporative losses from riparian species has not been sufficiently explored. This study focused on scaling up r_L to r_c for common reed, peachleaf willow, and cottonwood as a function of PPFD and other in-canopy radiation transfer parameters to estimate transpiration (TRP) rates of individual riparian species. We separated the modeled TRP from the Bowen ratio energy balance system (BREBS) measured total evapotranspiration using the corresponding individual species coverage data to quantify surface evaporation rates in a mixed riparian plant community in the Platte River Basin in central Nebraska.

2. Materials and Methods

2.1. Research Site and Vegetation Cover

[5] Extensive field campaigns were conducted during the study periods spanning from late April/early May through late October in 2009 and 2010 at a research site located in the Platte River Basin in central Nebraska near Central City, Merrick County, Nebraska ($41^\circ 7.939'N$; $97^\circ 55.52'W$; 507 m above mean sea level) (Figure 1). The experimental site is a sand bar island measuring 508 m long and 120–140 m wide with a northeast-southwest orientation in the Platte River formed at a braided area. The soil at the site is loamy sand (Gothenburg mixed, mesic typic psammaquents) with a particle size distribution of 87.5% sand, 10.3% silt and 2.2% clay with 0.064 m³ m⁻³ (vol %) field capacity, 0.016 m³ m⁻³ permanent wilting point, and 0.31 m³ m⁻³ saturation point. The bulk density is 1.82 g cm⁻³, and the saturated hydraulic conductivity is 32.4 $\mu\text{m s}^{-1}$ with negligible organic matter content [Irmak, 2010]. The site is

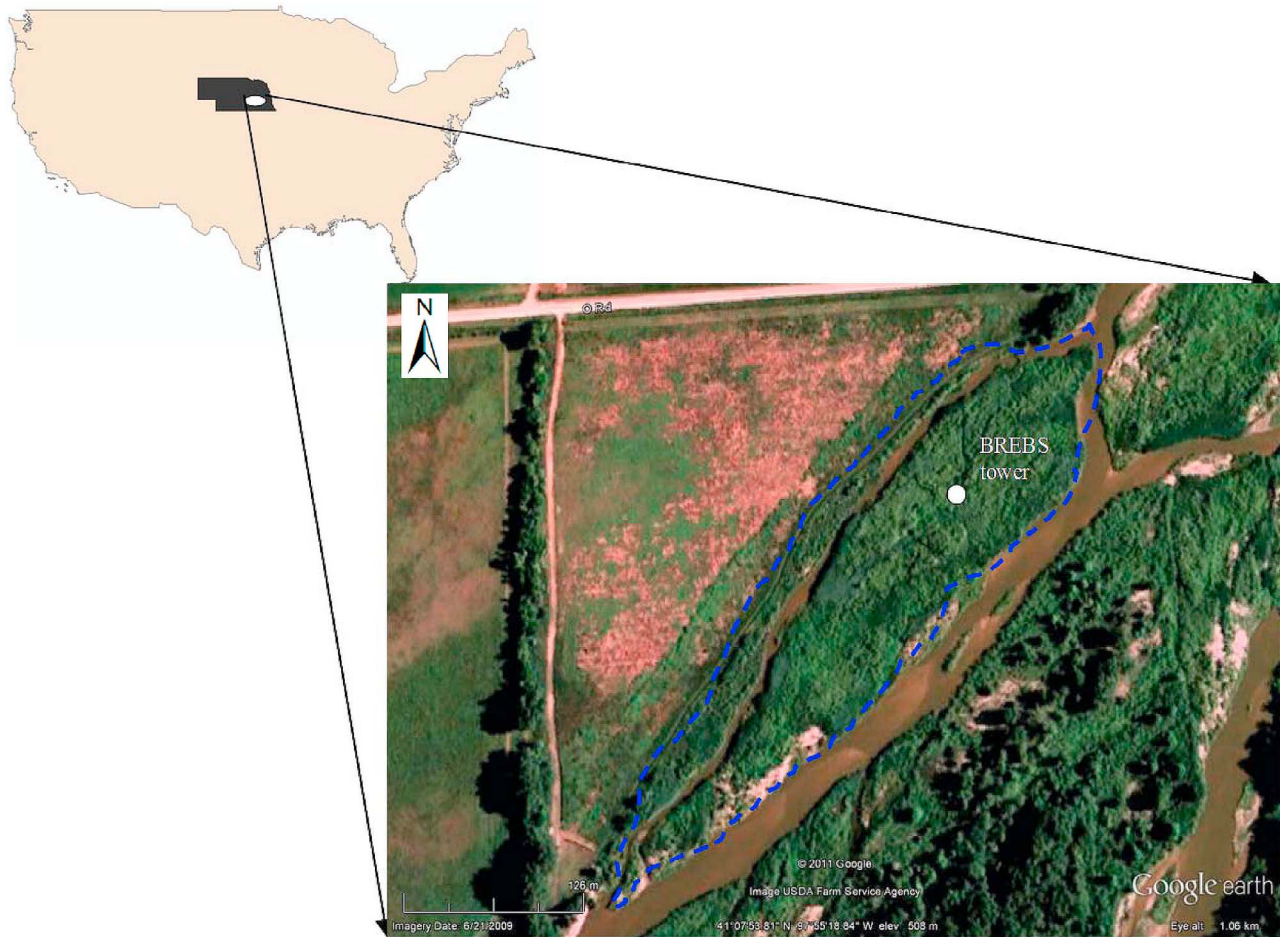


Figure 1. Location of the riparian plant community experimental island on the Platte River Basin near Central City, Nebraska (Google Earth, accessed on 9 January 2012).

dominated by common reed with vigorous vegetation canopy that covers the majority of the island during the active growing season. Based on extensive plant species composition of the experimental site and percent cover measurements conducted in 2010, several plant species were identified at the research site including, common reed (*Phragmites australis*), peachleaf willow (*Salix amygdaloides*), cottonwood (*Populus deltoides*), purple loosestrife (*Lythrum salicaria*), sand bar willow (*Salix exigua* subsp. *interior*), sedge (*Carex sp.*), reed canary (*Phalaris arundinacea*), swamp smartweed (*Polygonum amphibium*), wild indigo (*Amorpha fruticosa*), annual sunflower (*Helianthus annuus*), and common cattail (*Typha latifolia*). Common reed was the dominant species with 55.2% cover. Peachleaf willow and cottonwood had 29.3% and 6.7% cover, respectively. The other identified plant species occupied the remaining 7.8% of the experimental site with each individual species having a minor percent cover. Although the research site was composed of several other species, our research and measurements of surface energy balance, ET and TRP, physiological parameters, and their interactions focused on the three main species. Other species either had a very small spatial coverage or were present for a short portion of the growing season (June through early September). The two experimental years contrasted in terms of climate conditions as well as hydrological and surface conditions. In 2009, there was no

standing water on the island, and the soil surface was dry for the majority of the season, except on rainy days. However, several flooding events occurred in 2010 causing the presence of standing water on a large portion (close to 70–80%) of the island surface for a substantial portion of the growing season. The ponding water level on the island varied from 0.10–0.20 m to as high as 0.90 m from early June to late August.

2.2. Modified Step Point Method to Determine Plant Species Composition and Daubenmire Cover Class Method to Determine Vegetation Cover of the Experimental Site

[6] The plant species composition of the experimental site was determined on 30 July 2010 using a basal hit species composition method. The modified step point sampling procedure described by *Owensby* [1973] was followed to determine the plant species composition of the site. Two hundred sampling points (about 10 m apart) were placed on randomized transects throughout the experimental site. Despite being random, transects were systematically controlled to be in the NW-SE direction perpendicular to the general orientation of the island. The modified step point frame was lowered perpendicularly to the soil surface in front of the sampler's boot. The sampling point was offset from the initial ground contact of the frame to alleviate

subconscious placement of the sampler. Species recorded were those whose bases were in contact with the sampling point.

[7] Daubenmire cover class method is a widely used measure of percent cover of plant species because it is not biased by the size or distribution of individual species [Floyd and Anderson, 1987]. The canopy coverage technique by Daubenmire [1959] was used to estimate cover of each plant species on the island. A 0.20×0.50 m rectangle was used to outline 200 sampling plot placements about 10 m apart along randomized transects throughout the island. The coverage, interpreted as a vertical projection of a polygon drawn along the edges of the undisturbed canopy, was estimated separately for each species in each plot. The percentage of the rectangle's area covered by each plant species' canopy was assigned to one of six classes; 0–5, 5–25, 25–50, 50–75, 75–95, and 95–100% in the field. It was assumed that a plant species covered all the area within the horizontal boundary (outline) coverage of its canopy. Subsequently, midpoints of the cover classes (2.5, 15, 37.5, 62.5, 85, and 97.5%) were used to calculate the mean coverage using the assumption that actual cover values are uniformly distributed about the midpoints of each cover class. The percentage coverage relates the individual plant species to the total area of the island. If the sum of percentage coverage of different plant species is greater than 100%, then the canopy is composed of overlapping strata for the individual plant species.

2.3. Leaf Area Index and Plant Height Measurements

[8] The LAI for sunlit and shaded leaves of each plant species was measured using a model LAI-2000 plant canopy analyzer (LI-COR Biosciences, Lincoln, Nebraska). The LAI, in general, is defined as the one half the total green leaf area per unit ground surface area [Chen and Black, 1992; Chen *et al.*, 1997]. Because LAI-2000 is sensitive to all light-blocking objects in its view, it measures “foliage area index”, or more commonly known as effective LAI. In the case of woody trees, the LAI-2000 separates the woody portion of the canopy from the leaf area [LI-COR Biosciences, 2012]. LAI-2000 determines LAI from radiation measurements made with a “fish-eye” optical sensor (148° field of view). Because riparian systems are composed of heterogeneous and open-canopy structures, quantifying canopy structure with instruments/methods developed for homogeneous, closed-canopies (e.g., LAI-2000) may be prone to errors/challenges [Ryu *et al.*, 2010]. This potential issue is studied through a field campaign by Ryu *et al.* [2010], who examined the applicability of two direct (litterfall, allometry) and five indirect (LAI-2000, TRAC, digital hemispheric photography, digital cover photography, traversing radiometer) methods to determine LAI in an oak savanna ecosystem in California. They recommended that leaf inclination angle distribution should be characterized, and they provided a protocol to quantify LAI and its associated canopy structure variables in open-canopy ecosystems. The LAI-2000 calculates LAI from measured radiation transmittance (gap fraction) using inversion models that assume a random spatial distribution of leaves [Chen *et al.*, 1997]. While LAI-2000 provides accurate LAI measurements for agronomic crops and homogenous vegetation, it may not be able to “perfectly” represent the heterogeneous canopy LAI of natural ecosystems, such as clumped riparian vegetation. Chen *et al.* [1997] compared several methods for

determining LAI and reported that LAI-2000 may underestimate the LAI of boreal forest stands where the foliage is clumped. Their comparative study provided a comprehensive data set and analyses of LAI estimates available for boreal forests and demonstrated that optical techniques, combined with limited direct foliage sampling, can be used to obtain quick and accurate LAI measurements in such conditions. In our LAI measurements and data analyses, we did not account for the clumping effect. Measurements were made above and below the canopy to determine canopy light interception at the five angles from which LAI is computed using a model of radiative transfer in vegetative canopies [LI-COR Biosciences, 2012]. For each LAI value recorded, one reading above the canopy was taken and four other readings at different points within 1 m of each other were taken at the base of the canopy to sample variability within the canopy. LAI was measured at five locations on the island on a weekly basis. Two of the areas located south and northwest of the BREBS were dominated by common reed. One area that was dominated by peachleaf willow, and the other two areas dominated by cottonwood species were located east, northeast, and northwest of BREBS, respectively. The LAI measurement locations in which certain species were dominant were determined based on the plant species composition of the site and percent cover measurements. On average, about 40 LAI measurements were taken for common reed and cottonwood while 20–24 LAI measurements were taken for peachleaf willow on each measurement day. LAI was measured 17 times in both years. Thus, a total of 680 LAI measurements were made for common reed and cottonwood and about 374 measurements for the peachleaf willow in each year. To determine the rate of growth in plant height (h) for each species during the growing season, 10 common reed plants, three cottonwood trees, and eight peachleaf willow trees were marked, and their heights were measured every week throughout both seasons. The height was measured using a telescopic surveyor's ranging gauge. The height measurements were averaged into one value for each species for the measurement day. The daily and hourly LAI and h values were linearly interpolated from the weekly field measurements for the scaling-up process and TRP modeling.

2.4. Evapotranspiration and Climatic Variables Measurement

[9] The BREBS-measured surface energy flux data, including actual evapotranspiration (ET_{aBREBS}) and other data sets used in this study, are part of the Nebraska Water and Energy Flux Measurement, Modeling, and Research Network (NEBFLUX) [Irmak, 2010] that operates 11 BREBSs and eddy covariance systems over various vegetation surfaces ranging from irrigated and rainfed grasslands; irrigated alfalfa; rainfed switchgrass; irrigated and rainfed croplands (with different irrigation methods), including maize, soybean, winter wheat under different tillage and management practices, and seed maize cover crop rotation; to a riparian systems. The surface energy fluxes, including latent heat and sensible heat fluxes, and meteorological variables, including air temperature (T_a), relative humidity (RH), incoming shortwave radiation (R_s), wind speed and direction, and precipitation from riparian species, were measured using a BREBS installed in the middle of the experimental island. T_a and RH gradients were measured using two platinum resistance thermometers and monolithic

capacitive humidity sensors (REBS Models THP04015 and THP04016, respectively, Radiation and Energy Balance, Inc., Bellevue, Washington). The BREBS used an automatic exchange mechanism that physically exchanged the T_a and RH sensors between two heights above the canopy. The lower exchanger sensors level was maintained at an average height of ~ 1 m above the canopy throughout the season, and the distance between the upper and lower exchanger sensors was kept at a constant distance of 1 m. Incoming and outgoing shortwave radiations were measured simultaneously using REBS model THRDS7.1 double-sided total hemispherical radiometer. Net radiation (R_n) was measured using a REBS Model Q*7.1 net radiometer. Both radiometers were installed at 4.5–5.0 m above the surface. Ground heat flux (G) was measured using three REBS HFT-3.1 heat flux plates and three REBS STP-1 soil thermocouple probes. Each pair of soil heat flux plate and soil thermocouple was placed at a depth of 0.08 m below the soil surface in close proximity to each other. The heat storage above the soil heat flux plates was estimated, and measured G was adjusted for soil temperature and soil moisture content. The surface soil moisture content was measured using three REBS Model SMP soil matric potential sensors. The BREBS was installed on 28 April 2009 and was vigorously maintained and monitored on a weekly basis.

2.5. Stomatal Resistance and PPF Measurements

[10] A dynamic diffusion porometer (model AP4, Delta-T Devices Ltd., Cambridge, UK) equipped with an unfiltered GaAsp photodiode light sensor with a spectral response similar to photosynthetically active radiation was used to measure r_L and PPF for randomly selected, green, healthy, fully expanded leaves of common reed, peachleaf willow, and cottonwood. Detailed descriptions of porometer calibration, instrumentation specifications, field measurement protocols and procedures, and other details of the measurements are given by *Irmak et al.* [2008], *Irmak and Mutiibwa* [2010], and *Mutiibwa and Irmak* [2011]. During the porometer field measurements, the following variables were recorded for each leaf for each species: PPF ($\mu\text{mol m}^{-2} \text{s}^{-1}$) on the leaf, chamber temperature ($^{\circ}\text{C}$), leaf and chamber temperature difference ($^{\circ}\text{C}$), RH (%) at the canopy level and at four to six r_L (s m^{-1}) readings from each leaf. Four to six readings were taken from each leaf, and 4 to 6 leaves were sampled from each of the species on each measurement day. About 8 to 10 common reed and 3 or 4 peachleaf willow and cottonwood trees were sampled on each measurement day. The measurements were taken to represent the lower 25%, middle 50%, and upper 25% of the canopy profile because porosity of leaves differs from leaf to leaf and r_L of sunlit and shaded leaves is different [*Rochette et al.*, 1991; *Irmak and Mutiibwa*, 2009a, 2009b].

2.6. Scaling-Up Measured Leaf Level Stomatal Resistance to Canopy Resistance

[11] While scaling up r_L to r_c to estimate TRP rates for agronomic crops has been applied successfully, the application of this procedure to estimate TRP rates of individual riparian species is new and, thus, presents challenges. This is mainly due to complex vegetation/canopy structure of riparian systems and also due to substantially more complex nature of the interactions between the level of the homogeneity and heterogeneity of the vegetation and the surrounding boundary

layer characteristics and distribution of the different species in the mixed system. There may be differences in evaporative flux from a canopy whose species are uniformly distributed versus one where the canopy is clumped. The footprint of the flux tower that is used to measure the evaporative losses can be important in such conditions because of the wind speed and direction impact on mixing the microclimate above the evaporating surface. For instance, in a uniformly mixed canopy, the location of the evaporative losses would be immaterial to the resultant flux at the BREBS measurement point in terms of variability across the source of the evaporative losses region. However, in heterogeneous canopy where there are clumps of different species, if the wind direction is such that the air does not pass over a particular clump of a different species, then that species will have little or no control on the resultant evaporative flux. Thus, the fetch (footprint) of the flux tower can play an important role in the accuracy of the final value of the evaporative flux measured. As previously mentioned, the BREBS used in this study was installed on a riparian island that was 508 m long and 120–140 m wide with a northeast-southwest direction. The predominant wind direction in the experimental region is from southwest, and there is enough fetch distance (at least 254 m) in southwest direction to enable the air mass to flow over the mixed riparian system, representing the fluxes from clumped and uniform species, to provide accurate flux measurements. This fetch also minimizes the potential impact of the horizontal advection on BREBS measurements. Thus, we consider that the BREBS measurement heights of this study are within the boundary layer of the sources of the evaporative flux.

[12] In this research, measured r_L data for each species were scaled up to r_c by integrating procedures described by different studies, including those considered calculation of zenith angle [*Goudriaan*, 1977; *Walraven*, 1978; *de Wit et al.*, 1978; *Duffet-Smith*, 1979; *Norman*, 1982; *de Pury and Farquhar*, 1997; *Irmak et al.*, 2008; *Irmak and Mutiibwa*, 2010; *Mutiibwa and Irmak*, 2011]; partitioning of solar radiation into direct and diffuse photosynthetically active radiation or PPF [*Wang*, 1976; *Norman*, 1980, 1982; *Weiss and Norman*, 1985; *Irmak et al.*, 2008; *Irmak and Mutiibwa*, 2010; *Mutiibwa and Irmak*, 2011]; and using photosynthetic photo-partitioning LAI into sunlit (LAI_{Sun}) and shaded leaf area ($\text{LAI}_{\text{shaded}}$) [*Norman*, 1982, 1993; *Irmak et al.*, 2008; *Irmak and Mutiibwa*, 2010; *Mutiibwa and Irmak*, 2011]. For individual species, the r_c value per unit area was computed as the sum of LAI_{Sun} and $\text{LAI}_{\text{shaded}}$, weighted by their respective LAI [*Sinclair et al.*, 1976; *Rochette et al.*, 1991; *Irmak et al.*, 2008]. We used an integrated approach (Figure 2) of aforementioned procedures as described by *Irmak et al.* [2008] and *Mutiibwa and Irmak* [2011].

[13] In the scaling up, the transpirative losses can be overestimated when the Rubisco activity per unit ground area is taken as the sum of the activities per unit leaf area within the canopy. Thus, such a scaling-up process must consider the heterogeneous distribution of radiation within the canopy and the nonlinear response of transpiration to radiation [*de Pury and Farquhar*, 1997]. To account for heterogeneous distribution of radiation within the canopy, we divided the canopy into three classes and measured r_L to represent the lower 25%, the middle 50%, and the top 25% of the canopy through extensive and vigorously large r_L sampling schemes for each species throughout the season.

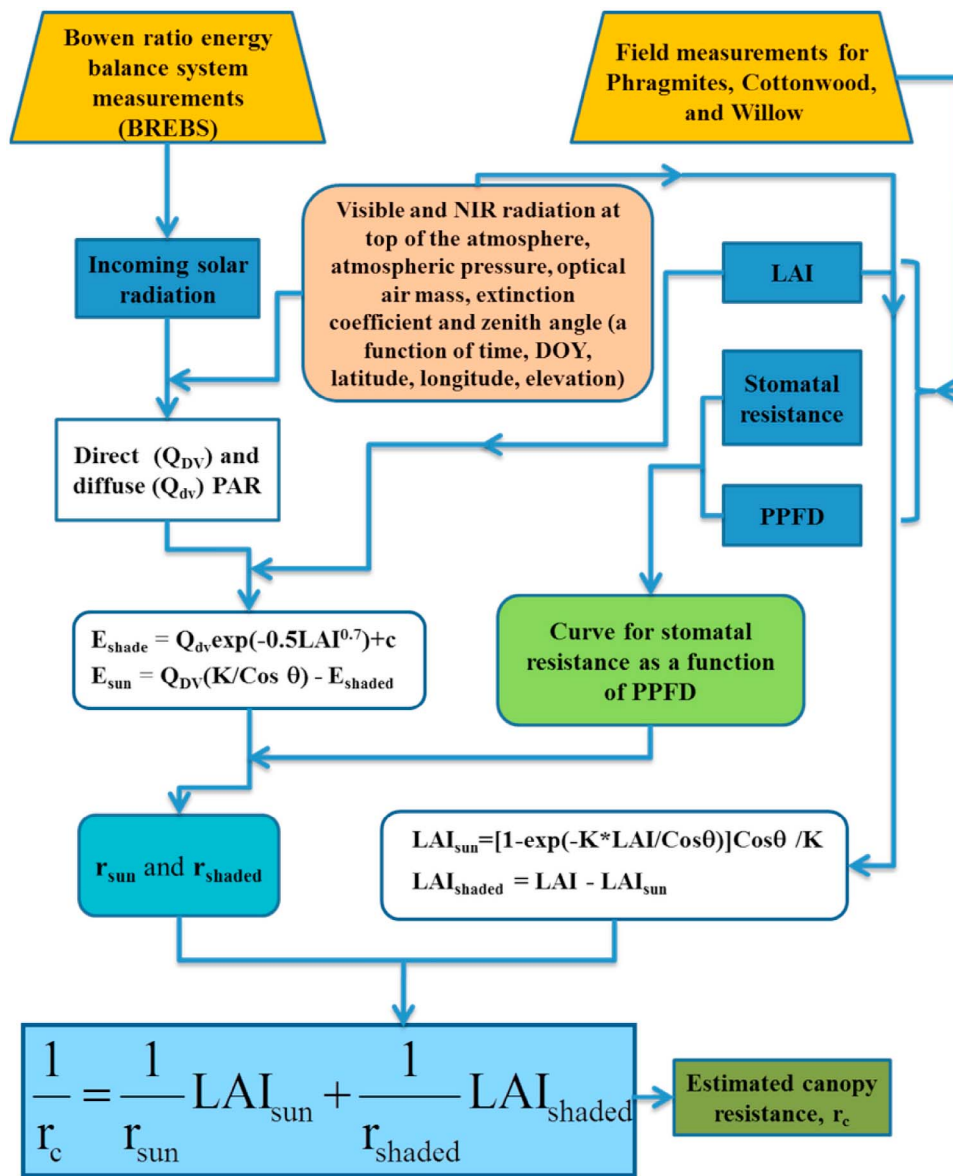


Figure 2. Schematic representation of the steps and primary equations used in the scaling-up field-measured leaf-level stomatal resistance (r_L) to canopy resistance (r_c).

This procedure is effective because transpiration of shaded leaves essentially has linear response to radiation, while transpiration of leaves in sunflecks is often light saturated, and is independent of radiation, allowing averaging of radiation in each of the three classes with little error in the final predicted canopy transpiration values [de Pury and Farquhar, 1997].

[14] The extensive process of scaling-up steps, procedures, and equations will not be repeated here, and readers are referred to detailed descriptions given by Irmak *et al.* [2008], Irmak and Mutiibwa [2010], and Mutiibwa and Irmak [2011]. The relationship between r_L and PPFD for the pooled data obtained through extensive r_L and within and above-canopy light interception measurements was used to determine r_L for the shaded and sunlit leaves during the scaling up r_L to r_c process. In our case, the experimental site was moisture-saturated throughout both seasons, so soil water was not limiting. The time-averaged TRP rates for

individual species were estimated using an evaporative diffusion model as a function of total canopy conductance (for individual species) and mean vapor pressure deficit [Tan *et al.*, 1978; Spittlehouse and Black, 1980; David *et al.*, 2004; Barradas *et al.*, 2005; Nicolás *et al.*, 2008]:

$$TRP = (\rho_a C_p / \gamma \lambda) g_T VPD \quad (1)$$

where TRP is time-averaged TRP ($\text{kg m}^{-2} \text{s}^{-1}$), ρ_a is the density of dry air (kg m^{-3}), C_p is the specific heat of dry air at constant pressure ($\text{J kg}^{-1} \text{°C}^{-1}$), ρ is the psychrometric constant (Pa °C^{-1}), λ is the latent heat of evaporation of water (J kg^{-1}), g_T is the total canopy conductance (m s^{-1}), and VPD is vapor pressure deficit (Pa). Total conductance was calculated based on the electrical analogue of a parallel circuit from r_c (s m^{-1}) and aerodynamic resistance (r_a , s m^{-1}) [Monteith, 1965; Monteith *et al.*, 1988; Monteith and Unsworth, 1990]. The canopy conductance values used in equation (1) for

Table 1. Daily Average Meteorological Parameters Measured During May–October at the Experimental Site^a

Meteorological Variable	May	Jun	Jul	Aug	Sep	Oct
2009						
u (m s ⁻¹)	2.3	1.5	1.2	1.3	1.1	1.9
T_{max} (°C)	22.8	24.9	26.4	25.9	22.5	11.6
T_{min} (°C)	10.5	15.4	15.0	14.7	10.8	2.2
RH (%)	66	80	80	81	78	79
R_s (W m ⁻²)	257	242	273	259	168	98
R_n (W m ⁻²)	152	155	176	167	106	53
VPD (kPa)	0.95	0.68	0.68	0.65	0.59	0.31
Rainfall (mm)	27	178	29	38	0	8
2010						
u (m s ⁻¹)	1.9	1.4	1.1	1.1	1.4	1.3
T_{max} (°C)	20.7	27.0	28.3	28.9	24.3	20.2
T_{min} (°C)	10.0	17.3	19.5	18.0	11.0	4.9
RH (%)	72	80	84	81	78	69
R_s (W m ⁻²)	243	276	268	262	183	161
R_n (W m ⁻²)	153	179	173	163	106	71
VPD (kPa)	0.73	0.75	0.63	0.75	0.70	0.76
Rainfall (mm)	81	163	120	96	34	14
Long Term (1987–2008)						
u (m s ⁻¹)	3.1	2.6	2.0	1.9	2.3	2.5
T_{max} (°C)	23.8	28.6	30.6	29.7	26.2	19.8
T_{min} (°C)	10.9	16.2	18.7	17.7	12.4	5.4
RH (%)	68	70	76	76	68	65
R_s (W m ⁻²)	220	256	254	220	182	129
R_n (W m ⁻²)	131	156	155	130	95	54
VPD (kPa)	0.94	1.15	1.04	0.97	1.07	0.81
Rainfall (mm)	120	94	91	70	72	50

^aWind speed (u), maximum and minimum air temperature (T_{max} and T_{min}), average relative humidity (RH), incoming shortwave radiation (R_s), net radiation (R_n), and monthly rainfall.

quantifying g_T were calculated using r_c (scaled up from measured r_L) and r_a above the canopy:

$$1/g_T = r_c + r_a \quad (2)$$

The computation of r_a was based on the assumption of a logarithmic wind profile [de Wit et al., 1978]:

$$r_a = \frac{\ln[(z_m - d)/z_{om}] \ln[(z_h - d)/z_{oh}]}{K^2 u_z} \quad (3)$$

where z_m is height of wind measurement (m), d is the zero plane displacement height (m), z_{om} is the roughness length governing transfer of momentum (m), z_h is height of humidity measurement (m), z_{oh} is the surface roughness length governing transfer of heat and water vapor (m), K is von Karman's constant (0.41), and u_z is wind speed at height z (m s⁻¹). The values of d , z_{om} (as a function of plant height, h (m)) and z_{oh} were calculated following de Wit et al. [1978]:

$$d = 0.67h \quad (4)$$

$$z_{om} = 0.123h \quad (5)$$

$$z_{oh} = 0.1z_{om} \quad (6)$$

The daytime total TRP values were estimated as the sum of the hourly values with a corresponding positive net radiation

(R_n) such that the daytime was defined as when the R_n value was greater than zero.

2.7. Estimation of Surface Evaporation

[15] Daily evaporation from the riparian zone was estimated using two methods: the difference between the daytime ET_{aBREBS} and the sum of the coverage-weighted TRP for the individual species. Considering that the research site had mixed vegetation species, hourly TRP for each individual species was weighted by the corresponding measured spatial coverage percentage. The second method estimated TRP as the difference between the daytime ET_{aBREBS} and the average of absolute TRP for the individual species. Thus, the estimated daily total evaporation values also include the TRP from the other species that had minor coverage at the experimental site. The two evaporation estimation procedures use daytime data to estimate daily total surface evaporation, and both methods assume that the nighttime transpiration values were small. From 30 April to 30 October, the BREBS-measured ET_{aBREBS} was 596 mm in 2009 and 840 mm in 2010. The nighttime evaporative losses (transpiration plus evaporation) that were measured with the BREBS were 16 mm in 2009 and 55 mm in 2010 (data are not shown). The nighttime was considered as when $R_s \leq 10$ W m⁻². Thus, the nighttime evaporative losses were only 3% and 6.5% of the daily (24 h) evaporative losses in 2009 and 2010, respectively. The nighttime evaporation losses were greater in 2010 primarily due to flooding.

3. Results and Discussion

3.1. Meteorological Conditions

[16] The monthly average (obtained from hourly data) meteorological variables measured by BREBS are presented in Table 1. For comparison, long-term (1987–2008) monthly average values of climate data for Central City are also included. The wind speed is usually greatest during spring and fall. On a seasonal average basis, 2010 was warmer and had greater R_s and lower wind speeds than 2009. The long-term average precipitation from May through October is 497 mm. Conditions in 2009, with only 280 mm precipitation, were much drier than long-term average conditions; they were also drier than 2010, which had 508 mm of growing season precipitation. The research site was flooded in 2010 with the water on the surface rising up to 0.90 m in June, July, and August.

3.2. Leaf Area Index and Plant Height

[17] The trends of measured LAI and h for each species in 2009 and 2010 are presented in Figure 3. LAI for common reed ranged from 1 to around 6 and peaked in late July to early August in both seasons. In 2009, the standard deviations (SD) of the LAI observations for common reed ranged between 0.1 and 0.6. In 2010, the SD ranged between 0.2 and 0.8 but was usually below 0.5 throughout the season. In July 2010, the plant growth rate for common reed was influenced by flooding as indicated by the leveling of h (Figure 3b). Flooding influences shoot growth by inhibiting internode elongation for common reed [Kozłowski, 1997]. We observed some stems attaining height as much as 3.7 m. The common reed height increased at a rate of 0.018 and 0.015 m d⁻¹ during May to early August in 2009 and 2010, respectively. The LAI for peachleaf willow

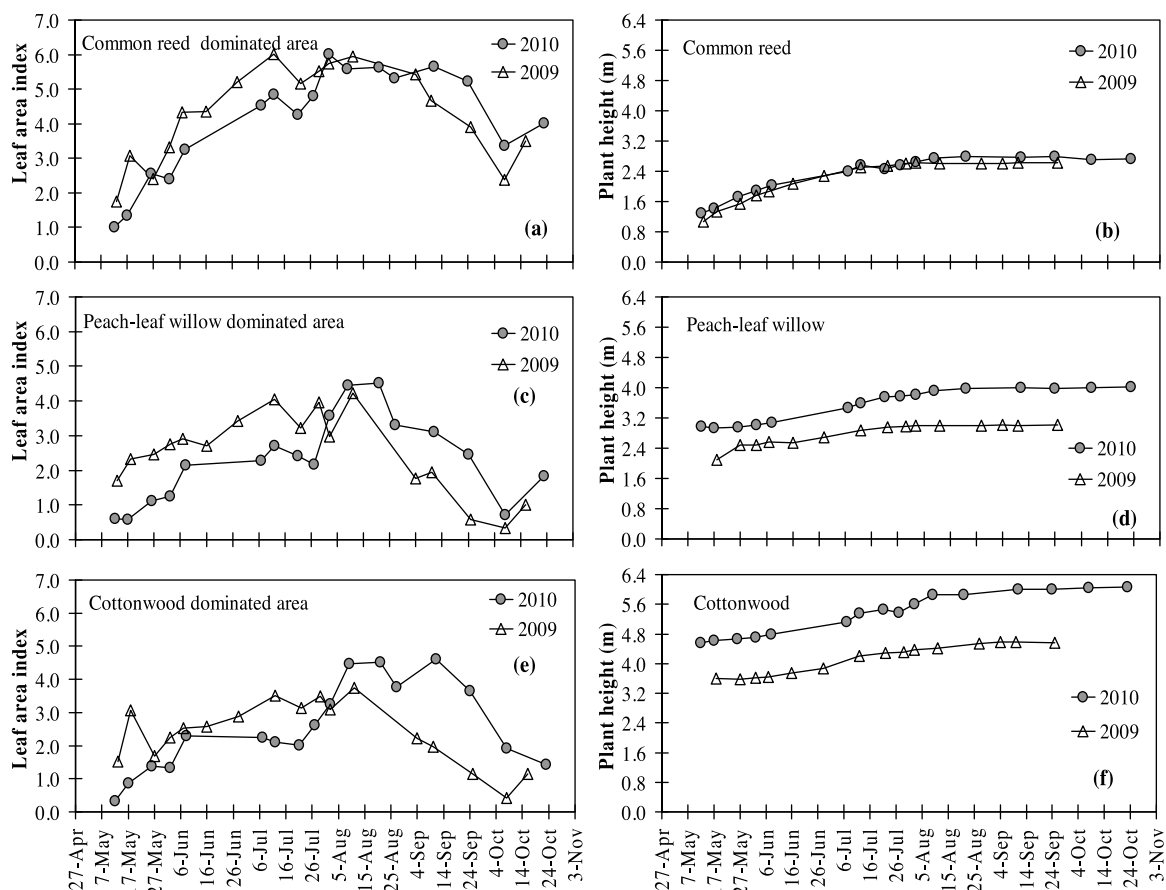


Figure 3. Seasonal trends of plant height (h) and leaf area index (LAI) for (a and b) common reed, (c and d) peachleaf willow, and (e and f) cottonwood during 2009 and 2010. Each data point represents an average of 8, 4, and 8 measurements from areas around the Bowen ratio energy balance system (BREBS) tower that were dominated by common reed, peachleaf willow, and cottonwood, respectively.

(Figure 3c) ranged between 1 and 5. We observed yellowing of peachleaf willow leaves in June and July due to flooding in 2010. The height for peachleaf willow (Figure 3d) increased at a rate of 0.010 and 0.012 m d^{-1} during May to early August in 2009 and 2010, respectively.

[18] In 2010, we observed yellowing of leaves in June and July and mortality of two cottonwood trees due to flooding. The LAI and h trends measured for cottonwood are given in Figures 3e and 2f, respectively. The cottonwood height increased at a rate of 0.012 and 0.014 m d^{-1} during May to early August in 2009 and 2010, respectively. The flooding in 2010 seems to have impacted all species as indicated by the lower h values during the first half of the season as compared with the corresponding values measured in the 2009 and a decrease in LAI in mid-July, during the peak of the flooding, followed by a steady increase. Flooding modifies shoot behavior and adversely influences shoot growth by inhibiting leaf initiation and leaf expansion, inducing premature leaf senescence, injury and abscission [Hook, 1984; Jackson and Drew, 1984; Kozłowski, 1997; Kozłowski and Pallardy, 2002]. We observed induced premature leaf senescence and abscission during flooding at the research site, which may explain the lower LAI values in the first half of the 2010 season, as compared with the same period in 2009.

3.3. Diurnal Trends of r_L and PPFD

[19] For all species, in 2009, diurnal trends of r_L and PPFD response curves at the leaf level were measured on 3 days (18 and 29 June and 11 August) and the diurnal response curve measurements were made on 26 July and 12 September 2010. There was a high variation in r_L and PPFD relationships for different leaves on the same plant for the same species. For example, on 18 and 29 June 2009, the SD of r_L and PPFD response curve data ranged between 12% and 31% and between 22% and 89%, respectively. In 2010, on 26 July and 12 September, average SDs of the response curves were 35% and 59% of the mean, respectively; r_L ranged between 73 s m^{-1} (PPFD = 1053 $\mu\text{mol m}^{-2} \text{s}^{-1}$) on 18 June at 13:00 LT and 187 s m^{-1} (PPFD = 235 $\mu\text{mol m}^{-2} \text{s}^{-1}$) measured on 11 August at 19:00 LT. On 18 and 29 June, r_L was consistently below 100 s m^{-1} but was greater than 100 s m^{-1} most of the day on 11 August. In 2009, we observed very small variations for r_L between 11:00 and 13:00 LT (18 June), 11:00 and 14:00 LT (19 June), and 10:00 and 11:00 LT (11 August), despite considerable changes in weather variables. The constant r_L under varying weather conditions suggests that during this period the water supply to the plant roots was equivalent to the transpiration loss.

[20] For peachleaf willow, in 2009, r_L ranged between 56 s m^{-1} (PPFD = 1204 $\mu\text{mol m}^{-2} \text{s}^{-1}$) on 18 June at

Table 2. Equations for the Relationship Between Leaf Stomatal Resistance (r_L) and Photosynthetic Photon Flux Density (PPFD) and Primary Weather and Plant Variables^a

Date	Equation ($y = r_L$; $x = \text{PPFD}$)	r^2	T ($^{\circ}\text{C}$)	RH (%)	u (m s^{-1})	VPD (kPa)	R_n (W m^{-2})	LAI	h (m)
<i>Common Reed (2009)</i>									
10 July	$y = 442.35x^{-0.296}$	0.73	24.9	91.7	1.26	0.31	124.2	5.84	2.45
14 July	$y = 1775.8x^{-0.52}$	0.89	23.9	83.2	1.42	0.66	193.7	5.93	2.50
21 July	$y = 403.38x^{-0.214}$	0.71	20.5	73.1	1.44	0.86	207.9	5.34	2.54
31 July	$y = 629.29x^{-0.309}$	0.81	18.10	73.4	1.28	0.91	201.9	5.58	2.62
28 Aug	$y = 457.08x^{-0.23}$	0.94	17.5	82.3	0.70	0.55	183.0	5.59	2.61
<i>Common Reed (2010)</i>									
9 June	$y = 1689.1x^{-0.64}$	0.95	20.8	73.8	0.64	0.95	210.5	3.24	2.03
13 July	$y = 8485.7x^{-0.731}$	0.91	25.4	84.1	1.62	0.74	190.3	4.84	2.56
22 July	$y = 1316.8x^{-0.45}$	0.86	27.1	83.3	1.30	0.78	205.7	4.25	2.47
5 Aug	$y = 1325x^{-0.421}$	0.81	22.4	82.9	0.41	0.64	169.2	5.89	2.67
11 Aug	$y = 740.09x^{-0.342}$	0.83	26.5	77.7	0.39	1.14	197.7	5.60	2.75
22 Aug	$y = 6480.1x^{-0.713}$	0.82	24.5	79.8	0.98	0.89	176.61	5.62	2.78
<i>Peachleaf Willow (2009)</i>									
10 July	$y = 3867.4x^{-0.592}$	0.83	24.9	91.7	1.26	0.31	124.2	3.92	2.83
21 July	$y = 859.67x^{-0.299}$	0.81	20.5	73.1	1.44	0.86	207.9	3.39	2.94
31 July	$y = 392.76x^{-0.242}$	0.82	18.1	73.4	1.28	0.91	201.9	3.71	2.98
28 Aug	$y = 999.69x^{-0.347}$	0.89	17.5	82.3	0.70	0.55	183.0	2.58	3.00
<i>Peachleaf Willow (2010)</i>									
9 June	$y = 3491.9x^{-0.762}$	0.94	20.8	73.8	0.64	0.95	210.5	2.15	3.07
13 July	$y = 24216x^{-0.898}$	0.90	25.4	84.1	1.62	0.74	190.3	2.70	3.58
22 July	$y = 1365.2x^{-0.343}$	0.88	27.1	83.3	1.30	0.78	205.7	2.41	3.75
5 Aug	$y = 735.7x^{-0.258}$	0.75	22.4	82.9	0.41	0.64	169.2	3.83	3.84
11 Aug	$y = 2067.9x^{-0.463}$	0.77	26.5	77.7	0.39	1.14	197.7	4.47	3.92
22 Aug	$y = 1283.4x^{-0.433}$	0.79	24.5	79.8	0.98	0.89	176.6	4.52	3.98
<i>Cottonwood (2009)</i>									
10 July	$y = 998.66x^{-0.307}$	0.74	24.9	91.7	1.26	0.31	124.2	3.92	2.83
21 July	$y = 868.19x^{-0.233}$	0.80	20.5	73.1	1.44	0.86	207.9	3.39	2.94
31 July	$y = 446.54x^{-0.207}$	0.88	18.0	73.4	1.28	0.91	201.9	3.71	2.98
28 Aug	$y = 505.52x^{-0.203}$	0.77	17.5	82.3	0.70	0.55	183.0	2.58	3.00
<i>Cottonwood (2010)</i>									
9 June	$y = 1349.1x^{-0.325}$	0.81	20.8	73.8	0.64	0.95	210.5	3.24	2.03
13 July	$y = 8375.9x^{-0.439}$	0.93	25.4	84.1	1.62	0.74	190.3	4.84	2.56
22 July	$y = 4437.4x^{-0.448}$	0.62	27.1	83.3	1.30	0.78	205.7	4.25	2.47
5 Aug	$y = 5541.1x^{-0.548}$	0.77	22.4	82.9	0.41	0.64	169.2	5.89	2.67
11 Aug	$y = 953.13x^{-0.340}$	0.83	26.5	77.7	0.39	1.14	197.7	5.60	2.75
22 Aug	$y = 19859x^{-0.893}$	0.73	24.5	79.8	0.98	0.89	176.6	5.62	2.78

^aIncludes air temperature (T), relative humidity (RH), wind speed (u), vapor pressure deficit (VPD), net radiation (R_n), leaf area index (LAI), and plant height (h) on the days of diurnal measurement in 2009 and 2010 for common reed, peachleaf willow, and cottonwood. r^2 = coefficient of determination.

13:00 LT and 234 s m^{-1} ($\text{PPFD} = 361 \mu\text{mol m}^{-2} \text{ s}^{-1}$) on 29 June at 18:00 LT. In 2010, r_L ranged between 157 s m^{-1} ($\text{PPFD} = 486 \mu\text{mol m}^{-2} \text{ s}^{-1}$) at 10:00 LT and 598 s m^{-1} ($\text{PPFD} = 951 \mu\text{mol m}^{-2} \text{ s}^{-1}$) measured at 18:00 LT on 26 July. On the 3 days of measurement in 2009, r_L for cottonwood ranged between 81 s m^{-1} ($\text{PPFD} = 1380 \mu\text{mol m}^{-2} \text{ s}^{-1}$) on 11 August and 356 s m^{-1} ($\text{PPFD} = 375 \mu\text{mol m}^{-2} \text{ s}^{-1}$) on 29 June at 18:00 LT. In 2010, cottonwood r_L ranged between 234 s m^{-1} ($\text{PPFD} = 543 \mu\text{mol m}^{-2} \text{ s}^{-1}$) and 400 s m^{-1} ($\text{PPFD} = 197 \mu\text{mol m}^{-2} \text{ s}^{-1}$) on 26 July and between 48 s m^{-1} ($\text{PPFD} = 389 \mu\text{mol m}^{-2} \text{ s}^{-1}$) and 407 s m^{-1} ($\text{PPFD} = 386 \mu\text{mol m}^{-2} \text{ s}^{-1}$) on 12 September.

3.4. Stomatal Resistance Versus PPFD Response Curves

[21] The field-measured r_L -PPFD response curves are the core of the scaling-up process to estimate TRP rates. Thus, in 2010, almost all of the diurnal r_L -PPFD response curves were measured when the experimental site was flooded with water level reaching up to 0.90 m. Following Irmak *et al.* [2008], we described the measured relationship between r_L

and PPFD by power functions in the form $r_L = k\text{PPFD}^n$. Our results showed that for all species, r_L increases sharply as PPFD decreases beyond $\sim 200 \mu\text{mol m}^{-2} \text{ s}^{-1}$. Table 2 presents the parameters of the relationships between r_L and PPFD for each species as well as weather and plant variables for each diurnal measurement days. The response curves for each species are discussed separately in sections 3.4.1–3.4.3.

3.4.1. Common Reed

[22] The 2009 and 2010 measured r_L and PPFD pooled data for common reed are presented in Figure 4a. Most of the r_L values greater than 400 s m^{-1} were measured during the flooding period in 2010 season. For common reed in 2009, the r^2 of the r_L -PPFD relationship varied between 0.71 and 0.94 (Table 2), suggesting a strong dependence of r_L on PPFD, and the pooled data in Figure 4a also had a high r^2 of 0.80; r_L began to increase sharply when PPFD decreased below $200 \mu\text{mol m}^{-2} \text{ s}^{-1}$. In contrast to 2009 data, in 2010 the stomata seem to have responded more strongly to PPFD between 400 and $800 \mu\text{mol m}^{-2} \text{ s}^{-1}$, resulting in lower r_L values for PPFD greater than $800 \mu\text{mol m}^{-2} \text{ s}^{-1}$. Thus, throughout the 2010 season, for PPFD values above

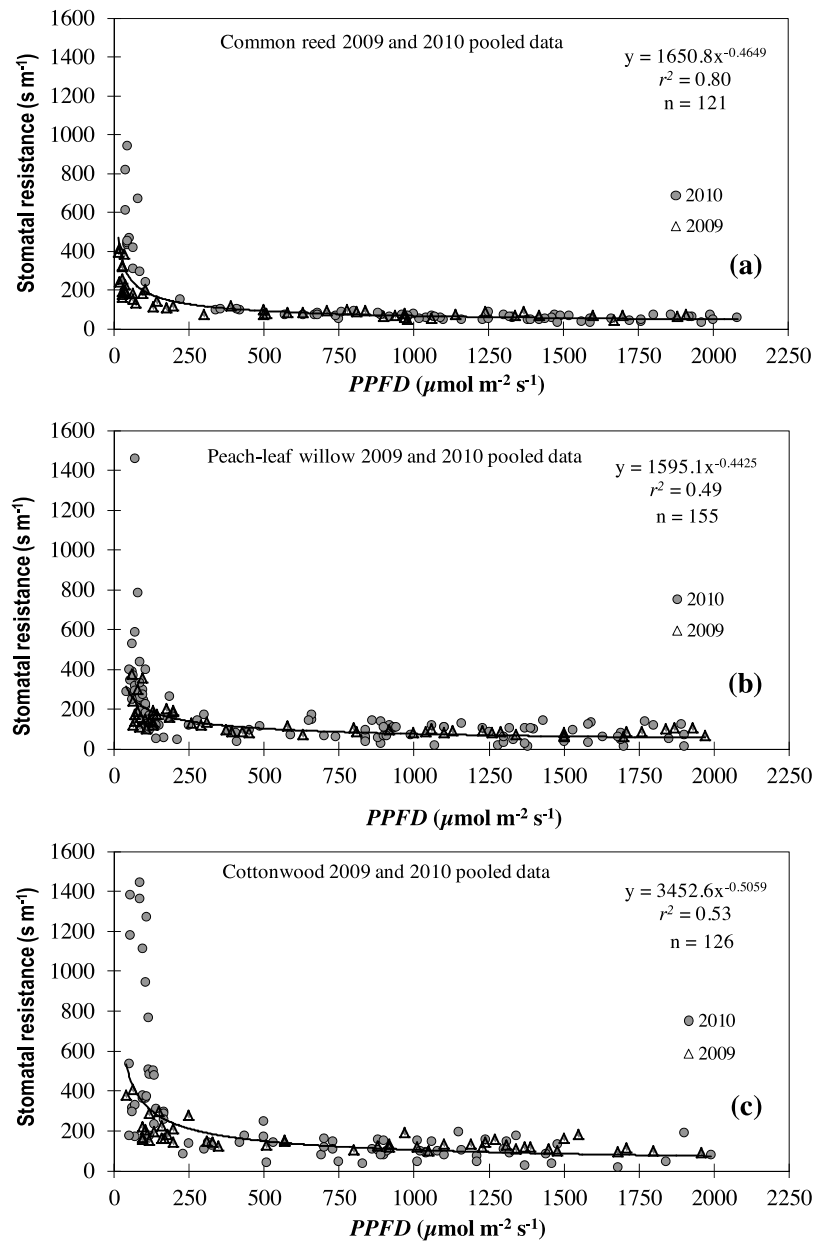


Figure 4. The 2009 and 2010 pooled response curves of measured stomatal resistance (r_L) as a function of photosynthetic photon flux density (PPFD) for (a) common reed, (b) peachleaf willow, and (c) cottonwood.

$400\ \mu\text{mol}\ m^{-2}\ s^{-1}$, r_L remained low and became less responsive to light. For all the measurement days, whenever PPFD was above $400\ \mu\text{mol}\ m^{-2}\ s^{-1}$, r_L varied between 24 and $101\ s\ m^{-1}$ with the greatest values occurring later in the season during leaf aging and/or leaf senescence stage, as was observed in 2009.

3.4.2. Peachleaf Willow

[23] For peachleaf willow, the r_L was more sensitive to PPFD at lower levels of PPFD than common reed and increased sharply below a PPFD value of $\sim 200\ \mu\text{mol}\ m^{-2}\ s^{-1}$. When PPFD was above $400\ \mu\text{mol}\ m^{-2}\ s^{-1}$, r_L varied between 60 and $100\ s\ m^{-1}$. The r^2 values for the relationships between r_L and PPFD were stronger than those observed for common reed, varying between 0.81 and 0.89 (Table 2), but the pooled data had lower r^2 (0.49) (Figure 4b). The lower r^2 for the pooled response curves for the peachleaf willow (and

cottonwood) is possibly due to the greater amount of variability in the measured r_L –PPFD relationships within the tree canopies that have greater heterogeneous canopy structures, resulting in more heterogeneous light penetration and distribution within the canopy, than common reed that have more uniform canopy orientation. Thus, for the peachleaf willow and cottonwood trees, there was more variability in r_L values for the same amount of light in the canopy, reducing the r^2 of the pooled r_L –PPFD relationship.

3.4.3. Cottonwood

[24] Although response curves had a similar form to those of common reed and peachleaf willow, curves for cottonwood had greater r_L values for similar PPFD than other two species. The r^2 of the r_L and PPFD relationships for cottonwood (Figure 4c) varied between 0.62 and 0.93 (Table 2) ($r^2 = 0.53$ for the pooled data, Figure 4c). For PPFD above

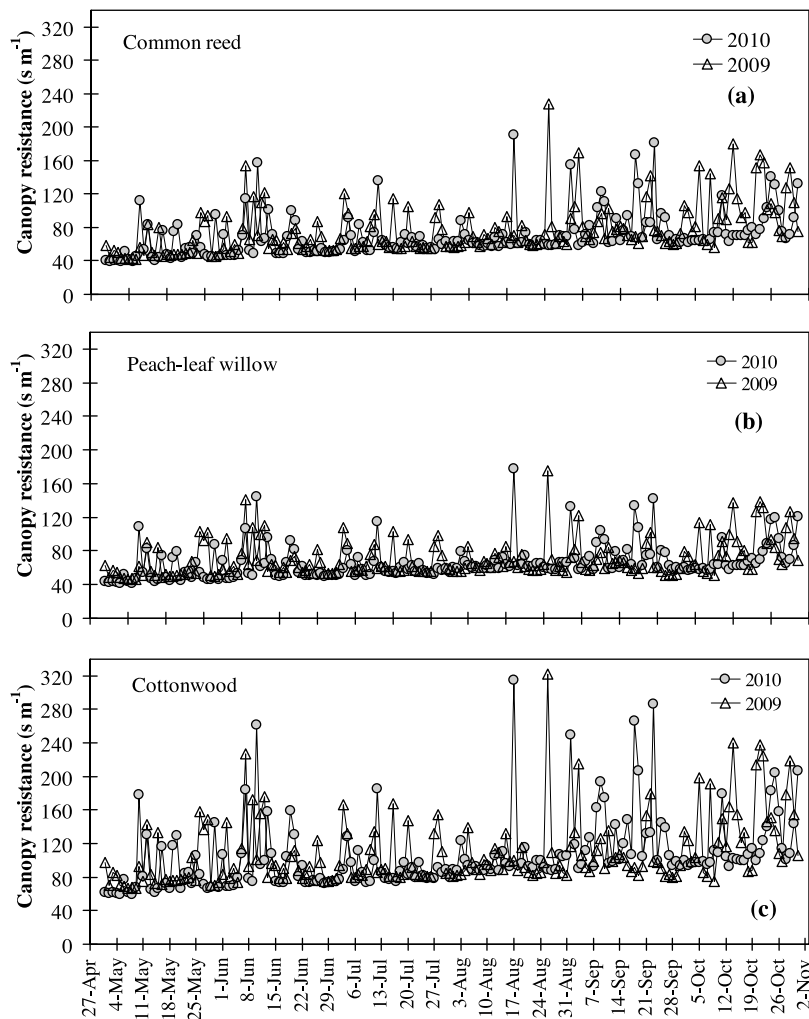


Figure 5. Average daytime canopy resistance (r_c) for (a) common reed, (b) peachleaf willow, and (c) cottonwood during the 2009 and 2010 growing seasons.

$400 \mu\text{mol m}^{-2} \text{s}^{-1}$, r_L became less responsive to light, but the magnitude varied widely between the diurnal measurement days. When $\text{PPFD} > 400 \mu\text{mol m}^{-2} \text{s}^{-1}$, r_L varied between 15 and 617 s m^{-1} . Most r_L values greater than 400 s m^{-1} in Figure 4c were measured during the flood year.

[25] Overall, the pooled data curves represented changes of the relationship between r_L and PPFD as the seasons progressed and implicitly integrated the impact of flooding and other environmental factors, leaf aging and senescence, various growth stages, and other factors during both growing seasons into the r_L versus PPFD relationship. The r^2 values (0.80, 0.49, and 0.53, for common reed, peachleaf willow, and cottonwood, respectively) of the pooled curves were less than the curves for individual measurement days for each species. Generally, the measured relationships between r_L and PPFD indicate that as light diffuses in the canopy r_L increases rapidly below a level of 200 to $300 \mu\text{mol m}^{-2} \text{s}^{-1}$. In addition to low PPFD, large r_L values observed in the pooled data curves could be a contribution of the mature/older leaves from the lower portion of the canopy or green leaves that receive less light in the lower canopy. Greater values of r_L from the middle part of the canopy could be a result of intracopy intermittent shedding that prevents leaves from equilibrating with PPFD [Katul et al., 2007]. On

the other hand, most of the low r_L values were from leaves in the upper part of the canopy or located such that they were in equilibrium and received maximum PPFD. As expected, days with higher VPD generally had higher r_L .

[26] In general, for all three species, whenever PPFD was above $400 \mu\text{mol m}^{-2} \text{s}^{-1}$, which corresponds to approximately one third of full sunlight, r_L remained low and became less responsive to light and varied between 40 and 108 s m^{-1} with the larger values occurring later in the season because of leaf aging and senescence. From these observations, there are distinctly different responses and sensitivity of the r_L to PPFD for two layers of the canopy: one that had sunlit leaves with low r_L and the other that had shaded leaves with high r_L values. The value of r_L never reached zero, indicating that there is always a physical limiting factor to water vapor flux exchange between the stomatal cavity and the surrounding microclimate. The observed high r_L value in July 2010 is most likely due to partial stomatal closure in response to flooding.

3.5. Seasonal Trend of Average Daytime r_c

[27] Seasonal daytime average r_c for common reed, peachleaf willow, and cottonwood during 2009 and 2010 are presented in Figures 5a, 5b, and 5c, respectively. For all the

Table 3. Seasonal Maximum, Minimum, and Average Canopy Resistance (r_c) for the Three Vegetation Species Studied During 2009 and 2010

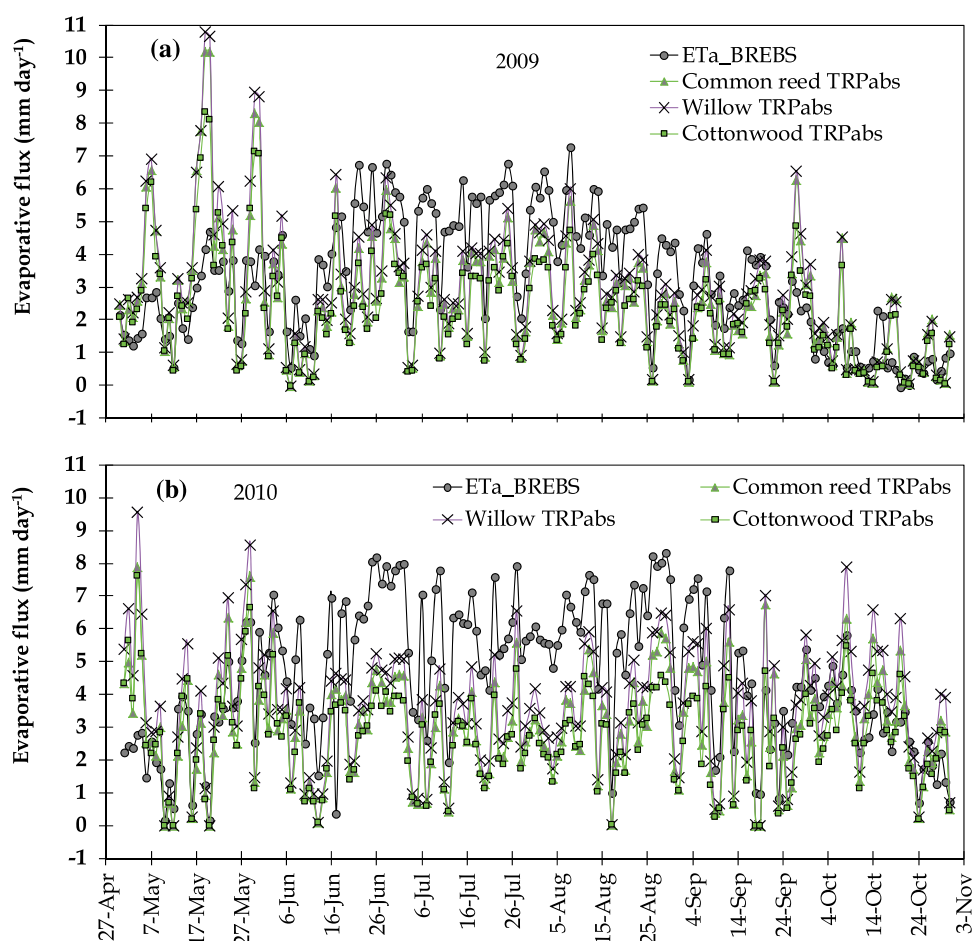
Vegetation Species	Canopy Resistance, r_c ($s\ m^{-1}$)					
	2009 Season			2010 Season		
	Maximum	Minimum	Average	Maximum	Minimum	Average
Common reed	228	41	76	191	39	70
Peachleaf willow	175	46	70	178	42	66
Cottonwood	322	66	107	315	59	105

species, r_c values were similar for both seasons (Table 3). The scaled-up minimum r_c values in our study are within the generalized summertime range of 40–100 $s\ m^{-1}$, as suggested by *McNaughton and Jarvis* [1983]. Excluding the days with maximum values, r_c had a steadily increasing trend from early season toward the end of the season with increased variability, particularly in 2010. Theoretically, r_c decreases with increasing irradiance but rises with increasing VPD as a result of partial stomatal closure. The irradiance was responsible for most of the variation in r_c during both seasons. For example, in 2009, r_c for common reed was 97 $s\ m^{-1}$ on 4 July ($R_s = 112\ W\ m^{-2}$) and decreased to 55 $s\ m^{-1}$ on 5 July ($R_s = 340\ W\ m^{-2}$) despite an increase in VPD from 0.15 to 0.72 kPa. The maximum r_c for all species occurred on 26 August 2009 and 17 August 2010. Both days

were cloudy and had low atmospheric evaporative demand. Daily average R_s and VPD values were 68 $W\ m^{-2}$ and 0.11 kPa for 26 August 2009 and 46 $W\ m^{-2}$ and 0.04 kPa for 17 August 2010, respectively. The r_c for peachleaf willow and cottonwood had a similar variation. Peachleaf willow and cottonwood, generally, had the lowest and greatest r_c values in both seasons, respectively.

3.6. Estimated Vegetation TRP Using Scaled-Up r_c

[28] In both years, TRP for peachleaf willow was usually greatest among all species (Figures 6a and 6b). In 2009, peachleaf willow TRP reached a maximum of 10.8 $mm\ d^{-1}$ with a seasonal average of 2.8 $mm\ d^{-1}$. The monthly average TRP rates for peachleaf willow were 4.4, 2.8, 3.1, 3.1, 2.5 and 1.1 $mm\ d^{-1}$ for May, June, July, August, September,

**Figure 6.** Seasonal trends of Bowen ratio energy balance system (BREBS) measured daily actual evapotranspiration (ETa_{BREBS}) and absolute plant transpiration ($TRPabs$) for common reed, peachleaf willow, and cottonwood in (a) 2009 and (b) 2010.

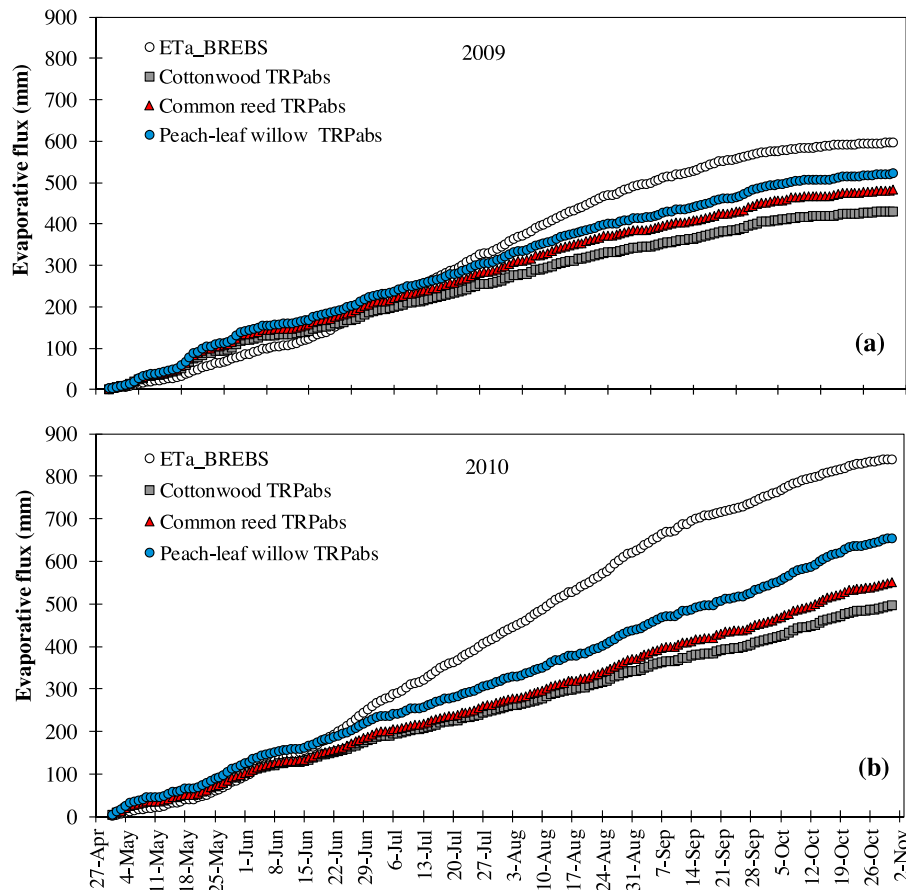


Figure 7. Seasonal cumulative trends of BREBS-measured daily actual evapotranspiration (ETa_{BREBS}), and absolute transpiration (TRPabs) for common reed, peachleaf willow, and cottonwood in (a) 2009 and (b) 2010.

and October, respectively. The seasonal average TRP values for common reed and cottonwood were 2.6 and 2.3 mm d^{-1} , respectively. The monthly average TRP rates for common reed were 4.1, 2.5, 2.9, 2.9, 2.2, and 1.0 mm d^{-1} for May, June, July, August, September, and October, respectively. The corresponding values for cottonwood were 3.7, 2.3, 2.5, 2.5, 2.2, and 0.9 mm d^{-1} , respectively. The 2009 seasonal total absolute TRPs for common reed, peachleaf willow, and cottonwood were 483, 522, and 431 mm, respectively (Figure 6a). Transpiration from the riparian zone contributed an average of 64% of ETa_{BREBS} during June–September with the proportion varying between 43% and 69% for most of the season.

[29] TRP for peachleaf willow in 2010 was also usually greatest of the three species and reached a maximum of 9.6 mm d^{-1} with a seasonal average of 3.6 mm d^{-1} . The monthly average TRP rates for peachleaf willow were 3.9, 3.4, 3.1, 3.8, 3.9, and 3.8 mm d^{-1} for May, June, July, August, September, and October, respectively, exhibiting less variability in monthly average TRP than other species. The 2010 seasonal average TRP for common reed was 3.0 mm d^{-1} , slightly greater than for cottonwood, and reached a maximum of 7.9 mm d^{-1} . The monthly average TRP rates for common reed were 3.2, 3.0, 2.6, 3.2, 2.8 and 3.1 mm d^{-1} , respectively. Cottonwood had the lowest seasonal average TRP of 2.7 mm d^{-1} with a maximum of

7.6 mm d^{-1} . The monthly average TRP rates were 3.1, 2.7, 2.4, 2.8, 2.3, and 2.7 mm d^{-1} , respectively. The 2010 seasonal total absolute TRP for common reed, peachleaf willow, and cottonwood were 550, 655, and 496 mm, respectively (Figure 7b). Figures 8a and 8b present the trends of the coverage-weighted TRP for each individual species during the 2009 and 2010 seasons, respectively. In both years, the seasonal total absolute TRP rates were greatest for peachleaf willow and least for cottonwood.

3.7. Riparian Zone Surface Evaporation

[30] The seasonal cumulative ETa_{BREBS} , average absolute TRP (TRP_{av}), and weighted TRP (TRP_{wt}) based on percent vegetation cover and the resulting evaporation in 2009 and 2010 are presented in Figure 9. The 2009 seasonal average evaporation based on the difference between ETa_{BREBS} and weighted TRP (Evaporation_ TRP_{wt}) was 0.81 mm d^{-1} with a maximum value of 3.1 mm d^{-1} observed on 12 July. The monthly average evaporation rates were -1.3, 1.5, 2.2, 2.0, 0.6, and -0.14 mm d^{-1} , respectively. The seasonal total evaporation estimated using the sum of TRP_{wt} for the vegetation species was 212 mm, which was reduced to 150 mm after factoring in the condensation (negative latent heat flux data). When the daytime absolute TRP (TRP_{abs}) of the three species was averaged, the 2009 season total value was 479 mm. The seasonal total evaporation estimated using the

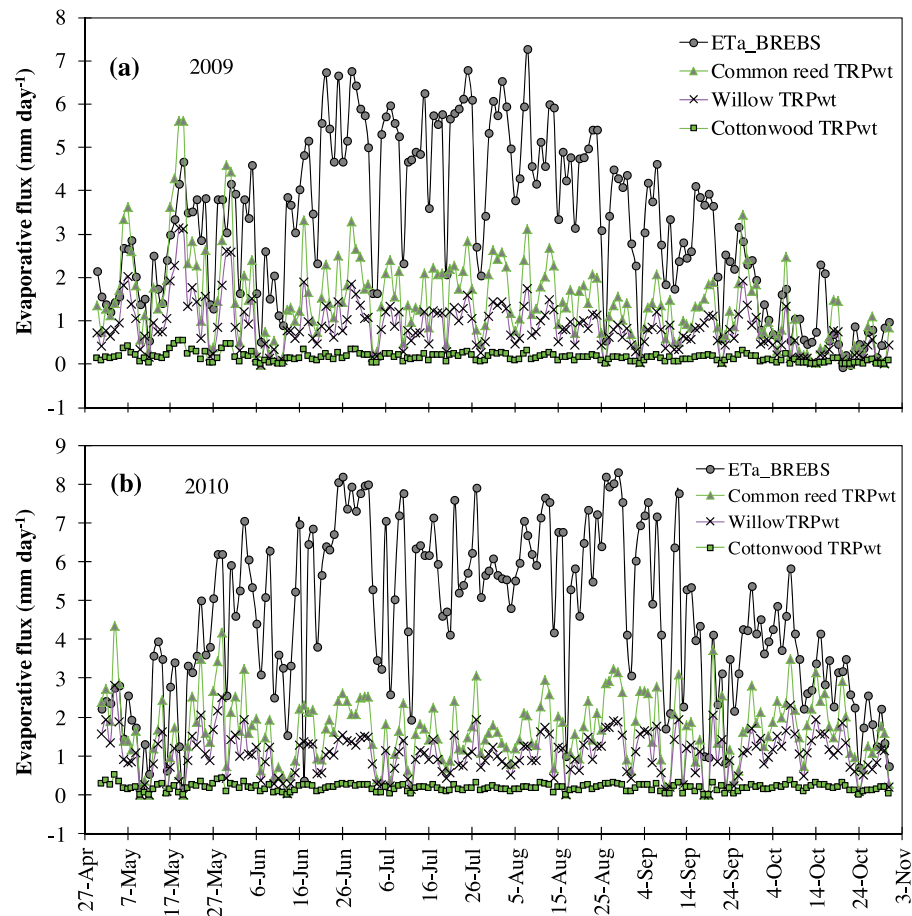


Figure 8. Seasonal trends of BREBS-measured daily actual evapotranspiration (ETa_{BREBS}) and species coverage proportion-weighted transpiration ($TRPwt$) for common reed, peachleaf willow, and cottonwood in (a) 2009 and (b) 2010.

average of absolute TRP for the vegetation species was 191 mm, which was reduced to 119 mm after factoring in condensation. The seasonal average evaporation in 2010 growing season was 1.70 mm d^{-1} with a maximum of 4.2 mm d^{-1} . The monthly average evaporation rates were $-0.2, 2.7, 3.2, 3.1, 1.6,$ and -0.01 mm d^{-1} , respectively. The 2010 seasonal total Evaporation_ $TRPwt$, estimated using the sum of $TRPwt$ for the all three vegetation species, was 349 mm, over one and a half times the value observed in 2009. Averaging the $TRPabs$ of the three species yielded a season total value of 567 mm. The seasonal total evaporation estimated using the average of absolute TRP for the vegetation species was 320 mm.

[31] Figure 10 presents the seasonal trends of ETa_{BREBS} ; total $TRPwt$ for cottonwood, common reed, and peachleaf willow; and the resulting evaporation in 2009 and 2010. The total $TRPwt$ from the three species was 448 and 528 mm in 2009 and 2010, respectively. The high atmospheric demand of some days early and late in the season resulted in TRP rates higher than ETa_{BREBS} , yielding negative evaporation (Figure 10a). Negative evaporation, in most cases, is an indication of condensation on the vegetation. At the beginning of the season, the negative evaporation is caused by the air temperature increasing more rapidly than the vegetation temperature due to the larger heat capacity of the vegetation. The negative evaporation, most likely, resulted from stable

thermal stratification caused by thermal inversion over the cooler vegetation [Gianniou and Antonopoulos, 2007].

4. Summary and Conclusions

[32] Riparian zones usually consist of a variety of vegetation species that have different TRP rates. This mosaic of vegetation presents a challenge for how to improve the accuracy of the evaporative flux estimates of individual species under such conditions. The challenge is compounded by the fact that riparian zones are often exposed to large fluctuations in environmental forcing and surface conditions throughout the growing season. Our study, one of the first, presents an integrated methodology to quantify evaporative losses (transpiration and evaporation) on an hourly basis for individual species in a common reed-dominated peachleaf willow and cottonwood mixed riparian plant community in the Platte River Basin in central Nebraska. With the espousal of the measured atmospheric parameters and environmental and plant factors as well as vegetation coverage data for individual vegetation species, the total evaporation from the riparian zone was estimated as the difference between measured ETa and modeled TRP . We scaled up r_L to r_c for individual species using microclimatic and plant variables. We measured r_L , LAI for sunlit and shaded leaves, h , solar zenith angle, direct and diffuse solar radiation for sunlight

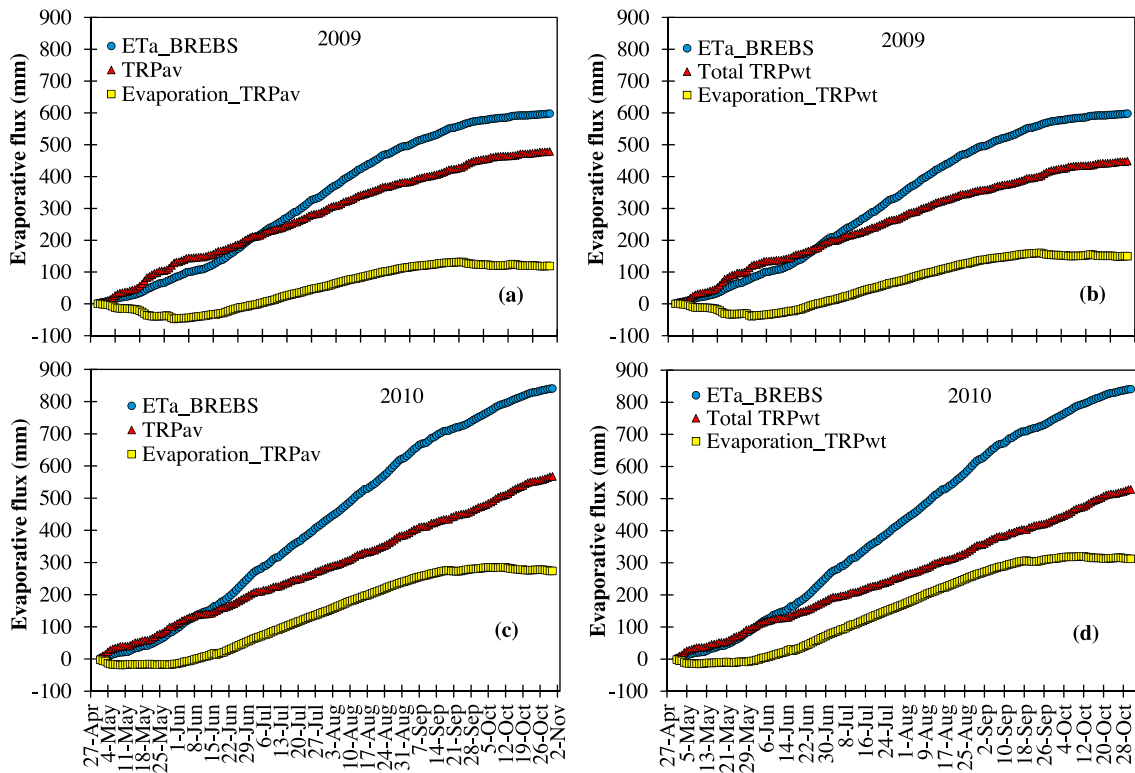


Figure 9. Seasonal cumulative BREBS-measured daily actual evapotranspiration (ET_{aBREBS}), the average of absolute transpiration (TRP_{av}), total species coverage proportion-weighted transpiration (TRP_{wt}) for common reed, peachleaf willow, and cottonwood, and riparian zone surface evaporation in (a and b) 2009 and (c and d) 2010.

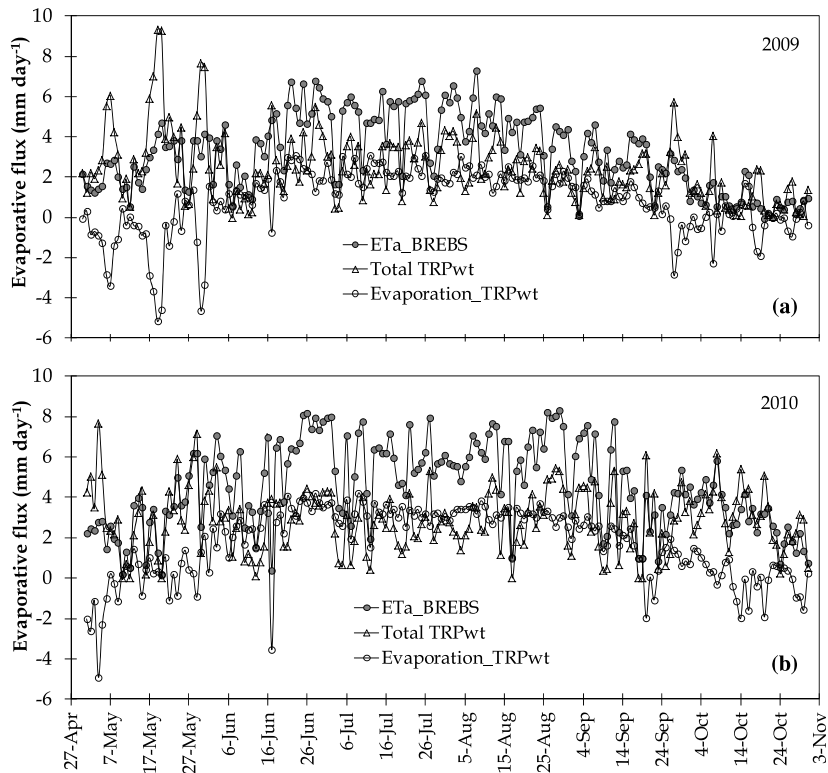


Figure 10. Seasonal trends of BREBS-measured daily actual evapotranspiration (ET_{aBREBS}), total species coverage proportion-weighted transpiration (TRP_{wt}) for common reed, peachleaf willow, and cottonwood, and riparian zone surface evaporation in (a) 2009 and (b) 2010.

and shaded leaves, and PPF_D and used an integrated within-canopy radiation physics approach to scale up r_L to r_c to model TRP. The main assumption in the scaling-up process was that the PPF_D is the primary driver of r_L when all other environmental factors, including soil water status, are not limiting. The relationship between r_L and PPF_D was described as a power function of the form $r_L = k\text{PPFD}^n$, and the relationships were asymptotic. Stomatal resistance was less responsive to PPF_D at higher PPF_D values ($>400 \mu\text{mol m}^{-2} \text{s}^{-1}$), whereas at lower PPF_D values ($<200 \mu\text{mol m}^{-2} \text{s}^{-1}$), r_L was very sensitive to PPF_D for all three species. Peachleaf willow and cottonwood, generally, had the lowest and greatest r_c values in both seasons, respectively. TRP was influenced by vegetation phenology (especially increase in LAI and leaf aging/leaf senescence) and strongly correlated with irradiance. Presence of flood water on the surface and warmer seasonal average temperatures (19°C in 2010 versus 17°C in 2009) contributed to the high evaporation rates observed in the 2010 growing season and affected vegetation physiological parameters and stomatal behavior. For mixed riparian vegetative surface, it is important to weight the TRP of the individual species by their corresponding spatial coverage to estimate the evaporation from the surface. The study provides valuable data for water-use rates of individual riparian plant species in a mixed plant community that can be used for more accurate water balance analyses. In addition, the study demonstrates that water-use rates of riparian species can be estimated using the integrated approach of scaling up r_L to r_c as the primary function of PPF_D. Further research is needed to validate this approach in quantifying TRP rates of riparian systems in different climatic regions that have different environmental forcings.

[33] **Acknowledgments.** The authors greatly appreciate the time and efforts of anonymous reviewers for reviewing the manuscript and for providing excellent and constructive comments that resulted in improvement of our manuscript. We also thank the editor, associate editor, and the Water Resources Research support staff for all their time and assistance during the review of this manuscript. We express our appreciation to the Central Platte Natural Resources District (CPNRD) for sponsoring this ongoing long-term experiment. We also extend our appreciation to Milton Moravek and Duane Woodward, from CPNRD, for their continuing help and support for this long-term project.

References

- Amsberry, L., M. A. Baker, P. J. Ewanchuk, and M. D. Bertness (2000), Clonal integration and the expansion of *Phragmites australis*, *Ecol. Appl.*, *10*, 1110–1118, doi:10.1890/1051-0761(2000)010[1110:CIATEO]2.0.CO;2.
- Barradas, V. L., E. Nicolás, A. Torrecillas, and J. J. Alarcón (2005), Transpiration and canopy conductance in Young apricot (*Prunus armenica* L.) trees subjected to different PAR levels and water stress, *Agric. Water Manage.*, *77*, 323–333, doi:10.1016/j.agwat.2004.09.035.
- Blossey, B. (1999), Before, during, and after: The need for long-term monitoring in invasive plant species management, *Biol. Invasions*, *1*, 301–311, doi:10.1023/A:1010084724526.
- Blossey, B., P. M. Schwarzländer, P. Häfliger, R. Casagrande, and L. Tewksbury (2002), Common reed, in *Biological Control of Invasive Plants in the Eastern United States*, Publ. FHTET-2002-04, edited by R. G. Van Driesche, et al., pp. 131–138, U.S. Dep. of Agric., For. Serv., Morgantown, W. Va.
- Chen, J. M., and T. A. Black (1992), Defining leaf area index for non-float leaves, *Plant Cell Environ.*, *15*, 421–429, doi:10.1111/j.1365-3040.1992.tb00992.x.
- Chen, J. M., P. M. Rich, S. T. Gower, J. M. Norman, and S. Plummer (1997), Leaf area index of boreal forests: Theory, techniques, and measurements, *J. Geophys. Res.*, *102*(D24), 29,429–29,443, doi:10.1029/97JD01107.
- Cleverly, J., C. Dahm, J. Thibault, D. McDonnell, and J. Coonrod (2006), Riparian ecohydrology: Regulation of water flux from the ground to the atmosphere in the Middle Rio Grande, New Mexico, *Hydrol. Processes*, *20*, 3207–3225, doi:10.1002/hyp.6328.
- Daubenmire, R. F. (1959), A canopy-coverage method of vegetational analysis, *Northwest Sci.*, *33*, 43–64.
- David, T. S., M. I. Ferreira, S. Cohen, J. S. Pereira, and J. S. David (2004), Constraints on transpiration from an evergreen oak in southern Portugal, *Agric. For. Meteorol.*, *122*, 193–205, doi:10.1016/j.agrformet.2003.09.014.
- de Pury, D. G. G., and G. D. Farquhar (1997), Simple scaling of photosynthesis from leaves to canopies without the errors of big-leaf models, *Plant Cell Environ.*, *20*, 537–557, doi:10.1111/j.1365-3040.1997.00094.x.
- de Wit, C. T., et al. (1978), *Simulation of Assimilation, Respiration and Transpiration of Crops*, 140 pp., Cent. for Agric. Publ. and Doc., Wageningen, Netherlands.
- Drexler, J., R. Snyder, D. Spano, K. Ta, and U. Paw (2004), A review of models and micrometeorological methods used to estimate wetland evapotranspiration, *Hydrol. Processes*, *18*, 2071–2101, doi:10.1002/hyp.1462.
- Duffet-Smith, P. (1979), *Practical Astronomy With Your Calculator*, 3rd ed., Cambridge Univ. Press, Cambridge, U. K.
- Furon, J., J. S. Warland, and W. Wagner-Riddle (2007), Analysis of scaling-up resistances from leaf to canopy using numerical simulations, *Agron. J.*, *99*, 1483–1491, doi:10.2134/agronj2006.0335.
- Gianniu, S. K., and V. S. Antonopoulos (2007), Evaporation and energy budget in lake Vegoritis, Greece, *J. Hydrol.*, *345*, 212–223, doi:10.1016/j.jhydrol.2007.08.007.
- Goodrich, D. C., et al. (2000), Seasonal estimates of riparian evapotranspiration using remote and in-situ measurements, *Agric. For. Meteorol.*, *105*, 281–309, doi:10.1016/S0168-1923(00)00197-0.
- Goudriaan, J. (1977), *Crop Micrometeorology: A Simulation Study*, Cent. for Agric. Publ. and Doc., Wageningen, Netherlands.
- Hook, D. D. (1984), Adaptations to flooding with fresh water, in *Flooding and Plant Growth*, edited by T. T. Kozlowski, pp. 265–294, Academic, Orlando, Fla.
- Irmak, S. (2010), Nebraska Water and Energy Flux Measurement, Modeling, and Research Network (NEBFLUX), *Trans. ASABE*, *53*(4), 1097–1115.
- Irmak, S., and D. Mutiibwa (2009a), On the dynamics of evaporative losses from Penman-Monteith with fixed and variable canopy resistance during partial and complete maize canopy, *Trans. ASABE*, *52*(4), 1139–1153.
- Irmak, S., and D. Mutiibwa (2009b), On the dynamics of stomatal resistance: Relationships between stomatal behavior and micrometeorological variables and performance of Jarvis-type parameterization, *Trans. ASABE*, *52*(6), 1923–1939.
- Irmak, S. and D. Mutiibwa (2010), On the dynamics of canopy resistance: Generalized linear estimation and relationships with primary micrometeorological variables, *Water Resour. Res.*, *46*, W08526, doi:10.1029/2009WR008484.
- Irmak, S., D. Mutiibwa, A. Irmak, T. J. Arkebauer, A. Weiss, D. L. Martin, and D. E. Eisenhauer (2008), On the scaling-up of leaf stomatal resistance to canopy resistance as a function of photosynthetic photon flux density, *Agric. For. Meteorol.*, *148*(6–7), 1034–1044, doi:10.1016/j.agrformet.2008.02.001.
- Jackson, M. B., and M. C. Drew (1984), Effects of flooding on growth and metabolism of herbaceous plants, in *Flooding and Plant Growth*, edited by T. T. Kozlowski, pp. 47–128, Academic, Orlando, Fla.
- Jarvis, P. G. (1976), The interpretation of the variations in leaf water potential and stomatal conductance found in canopies in the field, *Philos. Trans. R. Soc. London, Ser. B*, *273*(927), 593–610.
- Jarvis, P. G., and K. G. McNaughton (1986), Stomatal control of transpiration: Scaling up from leaf to region, *Adv. Ecol. Res.*, *15*, 1–49, doi:10.1016/S0065-2504(08)60119-1.
- Jones, H. G. (1992), *Plants and Microclimate*, 2nd ed., 428 pp., Cambridge Univ. Press, Cambridge, U. K.
- Katul, G. G., A. Porporato, and R. Oren (2007), Stochastic dynamics of plant–water interactions, *Annu. Rev. Ecol. Evol. Syst.*, *38*, 767–791, doi:10.1146/annurev.ecolsys.38.091206.095748.
- Knezevic, S. Z., A. Datta, and R. E. Rapp (2008), Noxious weeds of Nebraska—Common reed, *Nebr. Univ. Coll. Agric. Home Econ. Ext. Serv. Ext. Circ.*, *EC1668*.
- Kozlowski, T. T. (1997), *Responses of Woody Plants to Flooding and Salinity*, *Tree Physiol. Monogr.*, vol. 1, Heron, Victoria, B. C., Canada.
- Kozlowski, T. T., and S. G. Pallardy (2002), Acclimation and adaptive responses of woody plants to environmental stresses, *Bot. Rev.*, *68*, 270–334, doi:10.1663/0006-8101(2002)068[0270:AAAROW]2.0.CO;2.
- Lafleur, P. M. (2008), Connecting atmosphere and wetland: Energy and water vapor exchange, *Geogr. Compass*, *2*(4), 1027–1057, doi:10.1111/j.1749-8198.2007.00132.x.

- Lhomme, J. P., E. Elguero, A. Chehbouni, and G. Boulet (1998), Stomatal control of transpiration: Examination of Monteith's formulation of canopy resistance, *Water Resour. Res.*, *34*, 2301–2308, doi:10.1029/98WR01339.
- LI-COR Biosciences (2012), LAI-2000 user manual, Lincoln, Nebr.
- Mal, T. K., and L. Narine (2004), The biology of Canadian weeds. 129. *Phragmites australis* (Cav.) Trin. ex Steud, *Can. J. Plant Sci.*, *84*, 365–396, doi:10.4141/P01-172.
- McNaughton, K. G., and P. G. Jarvis (1983), Predicting effects of vegetation changes on transpiration and evaporation, in *Water Deficit and Plant Growth*, vol. VII, edited by T. T. Kozlowski, pp. 1–47, Academic, San Diego, Calif.
- Monteith, J. L. (1965), Evaporation and the environment, in *The State and Movement of Water in Living Organisms, XIXth Symposium, Swansea, Wales*, pp. 205–234, Cambridge Univ. Press, Cambridge, U. K.
- Monteith, J. L., and M. Unsworth (1990), *Principles of Environmental Physics*, 2nd ed., Edward Arnold, London.
- Monteith, J. L., G. S. Campbell, and E. A. Potter (1988), Theory and performance of a dynamic diffusion porometer, *Agric. For. Meteorol.*, *44*, 27–38, doi:10.1016/0168-1923(88)90031-7.
- Mutiibwa, D., and S. Irmak (2011), On the scaling-up of soybean leaf stomatal resistance to canopy resistance for one-step estimation of actual evapotranspiration, *Trans. ASABE*, *54*(1), 141–154.
- Nagler, P. L., E. P. Glenn, and T. L. Thompson (2003), Comparison of transpiration rates among saltcedar, cottonwood and willow trees by sap flow and canopy temperature methods, *Agric. For. Meteorol.*, *116*, 73–89, doi:10.1016/S0168-1923(02)00251-4.
- Nagler, P. L., R. L. Scott, C. Westenburg, J. R. Cleverly, E. P. Glenn, and A. R. Huete (2005), Evapotranspiration on western US rivers estimated using the enhanced vegetation index from MODIS and data from eddy covariance and Bowen ratio flux towers, *Remote Sens. Environ.*, *97*, 337–351, doi:10.1016/j.rse.2005.05.011.
- Nagler, P., A. Jetton, J. Fleming, K. Didan, E. Glenn, J. Erker, K. Morino, J. Milliken, and S. Gloss (2007), Evapotranspiration in a cottonwood (*Populus fremontii*) restoration plantation estimated by sap flow and remote sensing methods, *Agric. For. Meteorol.*, *144*, 95–110, doi:10.1016/j.agrformet.2007.02.002.
- Nicolás, E., V. L. Barradas, M. F. Ortuño, A. Navarro, A. Torrecillas, and J. J. Alarcón (2008), Environmental and stomatal control of transpiration, canopy conductance and decoupling coefficient in young lemon trees under shading net, *Environ. Exp. Bot.*, *63*, 200–206, doi:10.1016/j.envexpbot.2007.11.007.
- Norman, J. M. (1980), Interfacing leaf and canopy light interception models, in *Predicting Photosynthesis for Ecosystem Models*, vol. 2, edited by J. D. Hesketh and J. W. Jones, pp. 49–67, 304, CRC Press, Boca Raton, Fla.
- Norman, J. M. (1982), Simulation of microclimates, in *Biometeorology and Integrated Pest Management*, edited by J. L. Hatfield and I. J. Thomason, pp. 65–99, Academic, San Diego, Calif.
- Norman, J. M. (1993), Scaling processes between leaf and canopy levels, in *Scaling Physiological Processes Leaf to Globe*, edited by J. R. Ehleringer and C. B. Field, pp. 41–76, Academic, San Diego, Calif.
- Owensby, C. E. (1973), Modified step-point system for botanical composition and basal cover estimates, *J. Range Manage.*, *26*, 302–303, doi:10.2307/3896585.
- Peacock, C. E., and T. M. Hess (2004), Estimating evapotranspiration from a reed bed using the Bowen-ratio energy balance method, *Hydrol. Processes*, *18*, 247–260, doi:10.1002/hyp.1373.
- Potts, D. L., W. S. Harpole, M. L. Goulden, and K. N. Suding (2008), The impact of invasion and subsequent removal of an exotic thistle, *Cynara cardunculus*, on CO₂ and H₂O vapor exchange in a coastal California grassland, *Biol. Invasions*, *10*, 1073–1084, doi:10.1007/s10530-007-9185-y.
- Rochette, P., R. L. Desjardins, L. M. Dwyer, D. W. Stewart, and P. A. Dube (1991), Estimation of maize (*Zea mays* L.) canopy conductance by scaling up leaf stomatal conductance, *Agric. For. Meteorol.*, *54*, 241–261, doi:10.1016/0168-1923(91)90008-E.
- Ryu, Y., O. Sonnentag, T. Nilson, R. Vargas, H. Kobayashi, R. Wenk, and D. D. Baldocchi (2010), How to quantify tree leaf area index in an open savanna ecosystem: A multi-instrument and multi-model approach, *Agric. For. Meteorol.*, *150*(1), 63–76, doi:10.1016/j.agrformet.2009.08.007.
- Schaeffer, S. M., D. G. Williams, and D. C. Goodrich (2000), Transpiration of cottonwood/willow forest estimated from sap flux, *Agric. For. Meteorol.*, *105*, 257–270, doi:10.1016/S0168-1923(00)00186-6.
- Sinclair, T. R., C. E. Murphey, and K. R. Knoerr (1976), Development and evaluation of simplified models simulating canopy photosynthesis and transpiration, *J. Appl. Ecol.*, *13*, 813–829, doi:10.2307/2402257.
- Sonnentag, O., M. Detto, B. R. K. Runkle, Y. A. Teh, W. L. Silver, M. Kelly, and D. D. Baldocchi (2011), Carbon dioxide exchange of a pepperweed (*Lepidium latifolium* L.) infestation: How do flowering and mowing affect canopy photosynthesis and autotrophic respiration?, *J. Geophys. Res.*, *116*, G01021, doi:10.1029/2010JG001522.
- Spittlehouse, D. L., and T. A. Black (1980), Evaluation of the Bowen ratio/energy balance method for determining forest evaporation, *Atmos. Ocean*, *18*, 98–116, doi:10.1080/07055900.1980.9649081.
- Tan, C. S., T. A. Black, and J. U. Nnyamah (1978), A simple diffusion model of transpiration applied to a thinned Douglas-fir stand, *Ecology*, *59*(6), 1221–1229, doi:10.2307/1938235.
- Tourula, T., and M. Heikinheimo (1998), Modeling evapotranspiration from a barley field over the growing season, *Agric. For. Meteorol.*, *91*, 237–250, doi:10.1016/S0168-1923(98)00065-3.
- Walraven, R. (1978), Calculating the position of the Sun, *Sol. Energy*, *20*, 393–397, doi:10.1016/0038-092X(78)90155-X.
- Wang, W. C. (1976), A parameterization for the absorption of solar radiation by water vapor in the Earth's atmosphere, *J. Appl. Meteorol.*, *15*, 21–27, doi:10.1175/1520-0450(1976)015<0021:APFTAO>2.0.CO;2.
- Weiss, A., and J. M. Norman (1985), Partitioning solar radiation into direct and diffuse, visible and near-infrared components, *Agric. For. Meteorol.*, *34*, 205–213, doi:10.1016/0168-1923(85)90020-6.